ALGORITHMS FOR DETECTING AND SEGMENTING NUCLEATED BLOOD CELLS

by

STEVEN SUI-SANG POON, P.Eng.

B.A.Sc., The University of British Columbia, 1985

A THESIS SUBMITTED IN PARTIAL FULFILLMENT OF

THE REQUIREMENTS FOR THE DEGREE OF

MASTER OF APPLIED SCIENCE

in

THE FACULTY OF GRADUATE STUDIES

Department of Electrical Engineering

We accept this thesis as conforming

to the required standard

THE UNIVERSITY OF BRITISH COLUMBIA

August 1989

In presenting this thesis in partial fulfilment of the requirements for an advanced degree at the University of British Columbia, I agree that the Library shall make it freely available for reference and study. I further agree that permission for extensive copying of this thesis for scholarly purposes may be granted by the head of my department or by his or her representatives. It is understood that copying or publication of this thesis for financial gain shall not be allowed without my written permission.

Department of ELECTRICAL ENGINEERING

The University of British Columbia
Vancouver, Canada

Date Aug 21, 1989

Abstract

The analysis of the different types of cells in blood is routinely used in today's medical practice to give an indication of a person's state of health. Many imaging systems and algorithms have been developed over the last 30 years in an attempt to automate this process. Some of these systems can now distinguish the difference between normal and abnormal cells but the differentiation among the various types of abnormal cells is still undergoing active research.

A new system, the Cell Analyzer Imaging System, has been developed to acquire and process images from a microscope. In this work, some new algorithms have been developed using this system to detect and segment nucleated cells in Wright's stained blood smears for classification and sub-classification of the normal and abnormal cell types. The initial steps are to obtain high quality images by greatly reducing noise as well as by correcting distortions, aberrations and shading effects present in the acquired images. Spectral information from the images is then utilized to detect and segment nucleated cells from the rest of the scene (non-nucleated cells and background). All nucleated cells as well as those which are just touching are selected and separated into individual cells. The resulting single cells are further segmented into the regions of nucleus and cytoplasm. Simple features are then extracted from the segmented cells and these features are compared to determine if any clustering of a particular class of cell exists. Results show that these algorithms can detect, segment and classify

different types of normal and abnormal nucleated blood cells. The major errors in segmentation accounts for approximately 6% of the cells analyzed.

Table of Contents

List of Tables

List of Figures

Acknowledgements

I would like to thank all the staff and student members of the B.C. Cancer Research Centre who have assisted me in this thesis. I would specifically want to thank Dr. Bonnie Massing and Dr. Kamer Tezcan for their time and expertize in classifying more than 1000 blood cells. I would also like to express my gratitude to Joyce Mak for her time and patience in helping me with this documentation. Finally, I would like thank my supervisor, Dr. Rabab Ward, and my co-supervisors, Dr. Branko Palcic and Dr. Michael Beddoes, for their generosity in sharing their advice and time as well as their patience in allowing me to complete this work to my satisfaction. I am particularly in debt to Dr. Branko Palcic for the use of his facilities at the B.C. Cancer Research Centre in which I perform my experiments and research.

Chapter 1
Introduction

One of the most useful indicators of a person's state of health in today's medical practice is the examination of blood cells. The reason is that the production of the various types of blood cells (erythrocytes, leukocytes and platelets) in the body is highly sensitive to stress, injuries, diseases, poisons, ionizing radiation and other noxious stimuli (Zucker-Franklin et al., 1988; Begemann and Rastetter, 1979). The erythrocytes, commonly known as red blood cells, synthesize hemoglobin which is responsible for transporting oxygen and carbon dioxide to and from various parts of the body. The leukocytes or white blood cells are responsible for destroying and inactivating infective cells as well as for producing antibodies and other agents for the body's immune system. The platelets prevent bleeding by acting as agents to clot the blood on the surface of the wound. Thus the abnormality in the number of each type of cell in the blood sample as well as the irregularity in the morphology of the cells are important indications of the ill conditions under which they were produced (Zucker-Franklin et al., 1988; Begemann and Rastetter, 1979). This thesis is a study which leads to the development of algorithms for detecting and segmenting the various types of blood cells in single layer deposits of blood taken from patients. It is thought that the composition of the mixture of the blood cells is linked with the health of the patient.

A common technique of analysis is to visually examine the cells in a blood smear through a microscope (Figure 1). The smear is produced by spreading a thin film of blood over a glass slide which is then stained such that various features of the cell are enhanced for visual interpretation under the magnified field of a microscope. Wright's stain, developed in the 1800s, has become the standard stain for blood smear analysis (Zucker-Franklin et al., 1988; Begemann and Rastetter, 1979). The erythrocytes have no nucleus and when using Wright's stain, appear as light red in colour. The leukocytes have both nucleus and cytoplasm and are stained dark and light blue respectively. The platelets have only cytoplasm material and are stained light blue.

The visual interpretation and classification of these smears are subjective, tedious, time-consuming and susceptible to human error. In the diagnosis and classification of leukemia, there have been attempts made by the French-American-British (FAB) cooperative group (Bennett et al., 1976; Miller et al., 1981) to standardize the criteria for the division of the myeloid and lymphoid types as well as sub-classification within these types such that appropriate treatment can be prescribed. Although there is general acceptance of the classification scheme, the expense of this manual analysis and the inconsistencies in classification by observers among different institutions, as well as those in the same institution warrant some form of objective evaluation which can be used for diagnosis. This can be achieved by quantitative measurements of these cells using a semi or fully automated procedure. Since a large number of cells is generally measured, a fully automated

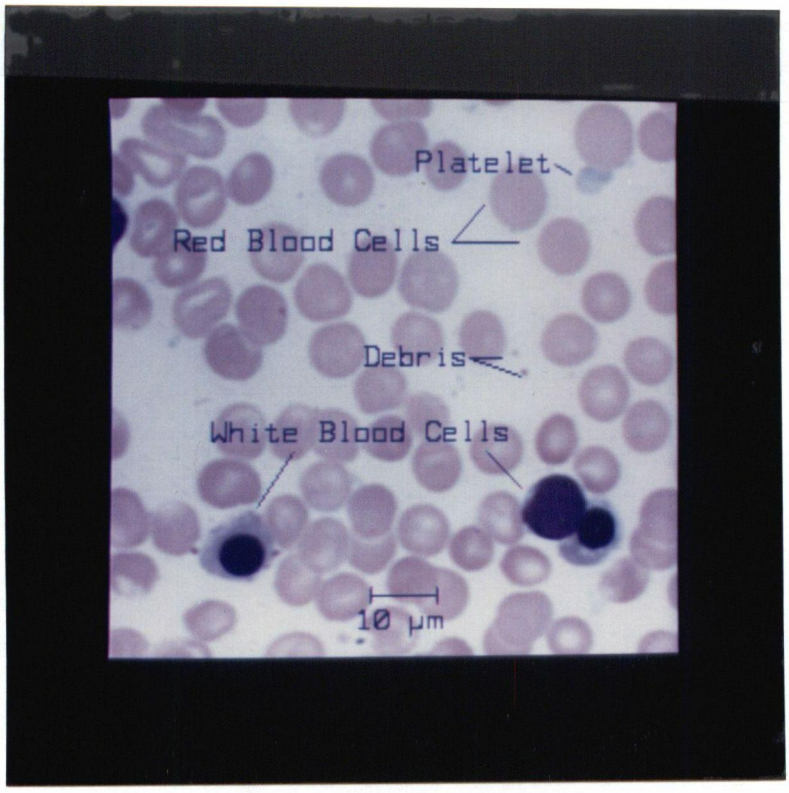

Figure 1

TYPICAL WRIGHT'S STAINED BLOOD SMEAR

A typical blood smear contains a) red blood cells, b) white blood cells, c) platelets, and d) debris. This photograph was taken at 40x microscope magnification.

system must eventually be developed if this approach is to be practically implemented.

The major deficiency of the commercially available cell analysis systems is their inability to differentiate the various types of abnormal cells. These commercial imaging systems were designed over the last ten to twenty years, and lack the quality of the transducers and optical components as well as the processing power which became available in the late eighties. In addition, the algorithms which involve the detection, segmentation, feature extraction and cell classification of different types of cells are still undergoing research.

The most difficult and also the most crucial step in an automated blood smear classification algorithm is that of correctly segmenting the image into its main components. These are the nucleus and the cytoplasm of the nucleated cells, the cytoplasm of the non-nucleated cells, and the background. Because of neurological processing which occurs in the eye, a human observer can easily determine and outline the various parts (nucleus and cytoplasm) of the cell in the image. A machine, however, has to resort to digital processing techniques to relate the set of pixels which make up the image, into distinct regions. Nonetheless, a machine can quantitatively describe the features extracted from these defined regions, a task which the human can only estimate using qualitative means. Any errors introduced in segmentation will propagate to feature extraction, object classification and will possibly lead to a misinterpretation of the cells in the scene. Therefore, correct

segmentation is of a paramount importance. However, the development of techniques for accurate and consistent segmentation of cells is not a trivial task.

This thesis is concerned with the software development of new algorithms for recognition, segmentation, feature extraction, and analysis of nucleated blood cells using a new image cytometry system, the Cell Analyzer which was designed and assembled to measure the properties of cells based on their images. These algorithms are computationally less expensive and match if not supercede the accuracy of those developed for other cytometry systems. The body of the thesis begins with the discussion of the characteristics of image cytometry systems in Chapter two. This section evaluates the systems currently used for analyzing blood cells and describes the system which is used to analyze the blood cells in this thesis. The discussion of some existing segmentation techniques is outlined in Chapter three. This section gives an indication of the different methods used by other researchers to segment the cells in the image. Parts of these methods are incorporated into the algorithms presented in Chapter four. New approaches for analyzing nucleated blood cells, such as the manipulation of the spectral information in segmenting nucleated cells, the separation of touching cells using the object chain code information and the angle of the tangent to the object boundary, and the filtering of the image using an edge enhancing average filter, are introduced in this chapter. The performance of these algorithms is examined in Chapter five.

Chapter 2
Automated Blood Analyzer

2.1 Image Cytometry Systems

The necessity for automation has led to the application of machine vision and robotics to microscopy in the early 1950s with the introduction of the blood cell analyzers (Young and Roberts, 1951; Walton, 1952). Since then, attempts have been made to automate other areas of medicine such as the screening of cervical cells (eg. Bengtsson et al., 1979; Tucker et al., 1979; Shoemaker et al., 1982) and the analysis of chromosomes (eg. Philip and Lundsteen, 1985; Preston, 1976). All these systems incorporate some type of a sensor for transforming the microscopic scene into a digital image, some robotics for bringing the area of interest on the microscope slide to the sensor's view, and a computer for analyzing the data and supervising the entire process. This technology has brought accuracy, uniformity, reproducibility, and a control level of quality to the performance of the screening programs.

The success of these automated cytometry systems can be seen by the commercial production of leukocyte analyzers by five different companies (three from the United States and two from Japan) in the last two decades (Preston, 1987; Imgram and Preston, 1970; Megla, 1973; Norgren, Kulkarni and Graham, 1981). These analyzers (eg. Hematrak by Smith Kline Beckman, LARC by Corning Glass Works, and diff3 by Coulter Electronics) have superior performance over humans in classifying the

slides as normal or abnormal but lack the capabilities in differentiating the different types of abnormal cells. Because of this deficiency and economical reasons, the three companies in the United States have stopped their production by 1986. Despite the lack of industrial interest, there is still active research in automating the analysis of abnormal blood cells by groups such as Palcic and Jaggi (1989) in Canada, Bacus and Grace (1987) in the United States, Aus et al (1986) and Haussmann and Liedtke (1984) in Germany, and Landeweerd et al (1983) in the Netherlands.

2.2 Flow Cytometry Systems

The analysis of cells using the fluid-flow technology (Fulwyler, 1965; Tyrer and Pressman, 1987) started in the 1960s. Fluid suspension is made into tiny droplets and cells in the droplets are passed through an interrogation orifice at high speeds (5000 cells/s). A cell can be examined while it passes through a field of view in approximately four microseconds. Laser light is shone at the droplets, which may contain the cell, and the transmittance and fluorescence at various wavelengths of light are measured. The data is transferred to a computer and processed. These systems presently are not capable of differentiating as many types of white blood cells as good image cytometry systems. However, the development of new immunologically based biochemical reagents, which tag the different classes of blood cells, may overcome this problem. With these new markers, the flow systems could be ideal for screening samples quickly and recognizing the rare abnormal cells

accurately. Since they do not allow visual observation of the cells detected, a blood smear must be made when an abnormal sample is detected for verification purposes.

2.3 General Imaging System Design

Although many image cytometry systems have been developed, they are very similar in design and operation. The basic system consists of an illumination source, microscope optics, motorized mechanical stage, camera, digitizing circuitry, image memory, display monitor, and processors (Figure 2). The stage which holds the samples is capable of moving objects in the X and Y direction to the detectors field of view. Z direction is provided for focussing purposes. Light is transmitted from the illumination source through the sample to the camera detector. The detected image is transformed into a digital image by the interfacing circuitry. The resulting digital image is stored in the computer memory from where it can be displayed on the monitor and/or processed and analyzed by the computer.

The major difference among these imaging systems is the transducer employed and the method used in scanning. Most systems use a two dimensional detector such as those found in tube cameras or a two dimensional array charge coupled device (CCD) cameras (eg. Jaggi et al., 1988; Tucker, 1979). The image is captured by the detector while the stage scans the slide by moving the sample from one frame to the next. Very few systems use a linear detectors such as diode or CCD arrays (eg.

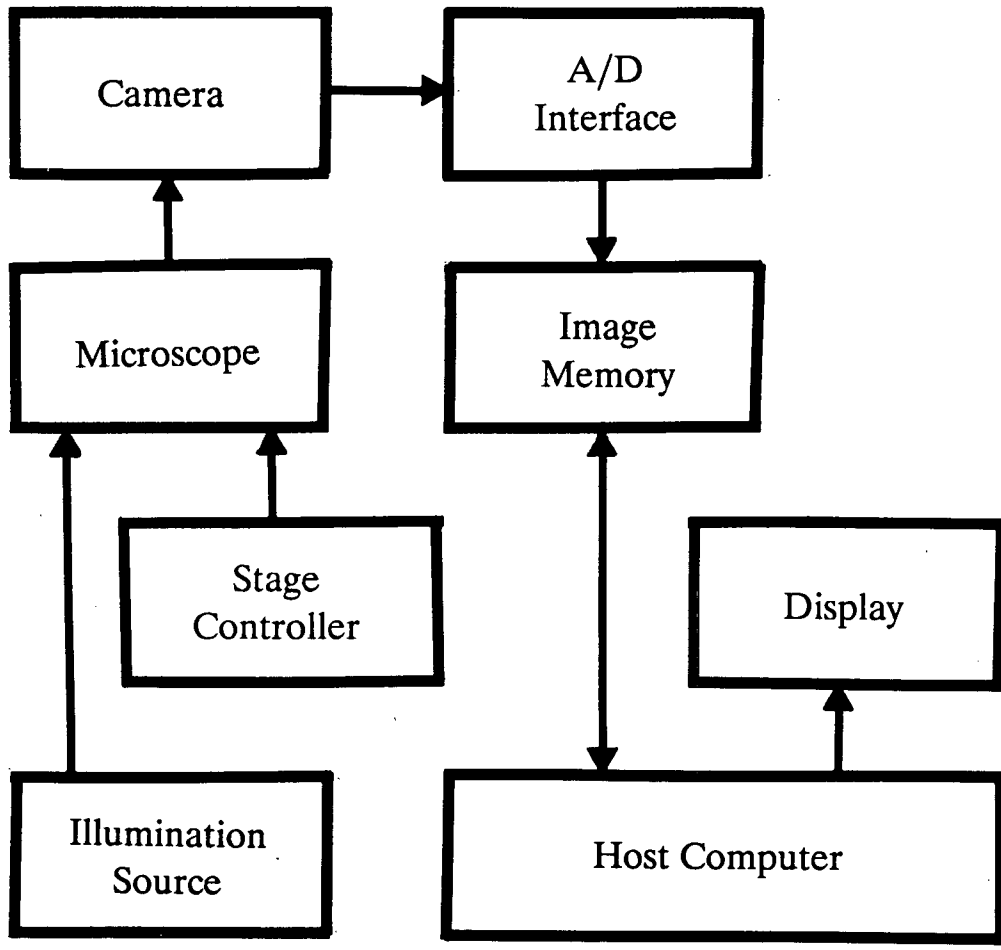

Figure 2

BLOCK DIAGRAM OF A TYPICAL IMAGE CYTOMETRY SYSTEM

A typical system consists of an illumination source, microscope, motorized stage, digitizing circuitry, image memory, display monitor and processors.

Jaggi and Palcic, 1985; Bengtsson et al., 1979; Tucker et al., 1987). In these systems, an image is obtained by moving the sample across the sensor and piecing together the image lines. The advantage of linear scanners is that they have more sensor elements than either a row or a column of the two dimensional counterpart and hence provide a wider field of view. Also, the elements of the sensor are digitized and stored as digital data, and not in a video (analogue) format which requires re-sampling to convert to a digital form. The major disadvantage is that a precise mechanical scanning is required for high resolution of the two-dimensional images. There are systems which use a combination of the linear and matrix (video) detectors (eg. Graham and Norgen, 1980). Objects detected by the linear array are moved into the field of view of the two dimensional detector for high resolution image acquisition. There are also systems which use a one element detector such as a photomultiplier or photodiode (eg. Ingram and Preston, 1970; Shoemaker et al., 1982). A rotating polygon is used to deflect the laser spot to scan the object in one dimension while the stage is moved to scan the image in the other dimension.

The quality of the input image in imaging is dependent not only on the type of transducers used but also on the optical components and electronic (digitizing) circuitry. The most important component in the optical system is the objective lens of the microscope which determines the magnification of the sample and hence governs the sampling density of the image. These lenses are not perfect and generally introduce distortions, aberrations, and shading effects. Most cameras today are

built for the television broadcast community where the detected image on the transducer is converted to an analog signal. This signal is later digitized for machine analysis resulting in a loss of information due to resampling and quantization errors. Cameras which directly digitize the sensor image into digital data for machine analysis are expensive and do not conform to a fixed standard of data transmission which results in the dependancy on a particular manufacturer for future upgrades. Distortions introduced by the optics, transducer and digitizing circuitry must be compensated for before the image can be analyzed.

2.4 Cell Analyzer Imaging System

The Cell Analyzer Imaging System was used to develop and test algorithms used for segmenting the blood smears described in this thesis. The Cell Analyzer was originally designed at the British Columbia Cancer Research Centre for the measurement of live, unstained cells to study their properties as a function of time and/or treatments (Palcic, Jaggi and Nordin, 1987). The description of this initial design is described elsewhere (Jaggi and Palcic, 1985; Jaggi, Poon and Palcic, 1986). A block diagram of the current system is shown in Figure 3 and 4. A two-dimensional CCD camera, frame grabbing and image processing board, and colour display monitor was added to the original system for measurements of stained cells (Jaggi et al., 1988). In addition to live cell experiments, this system is currently being used for the development of automatic segmentation and feature extraction algorithms of stained

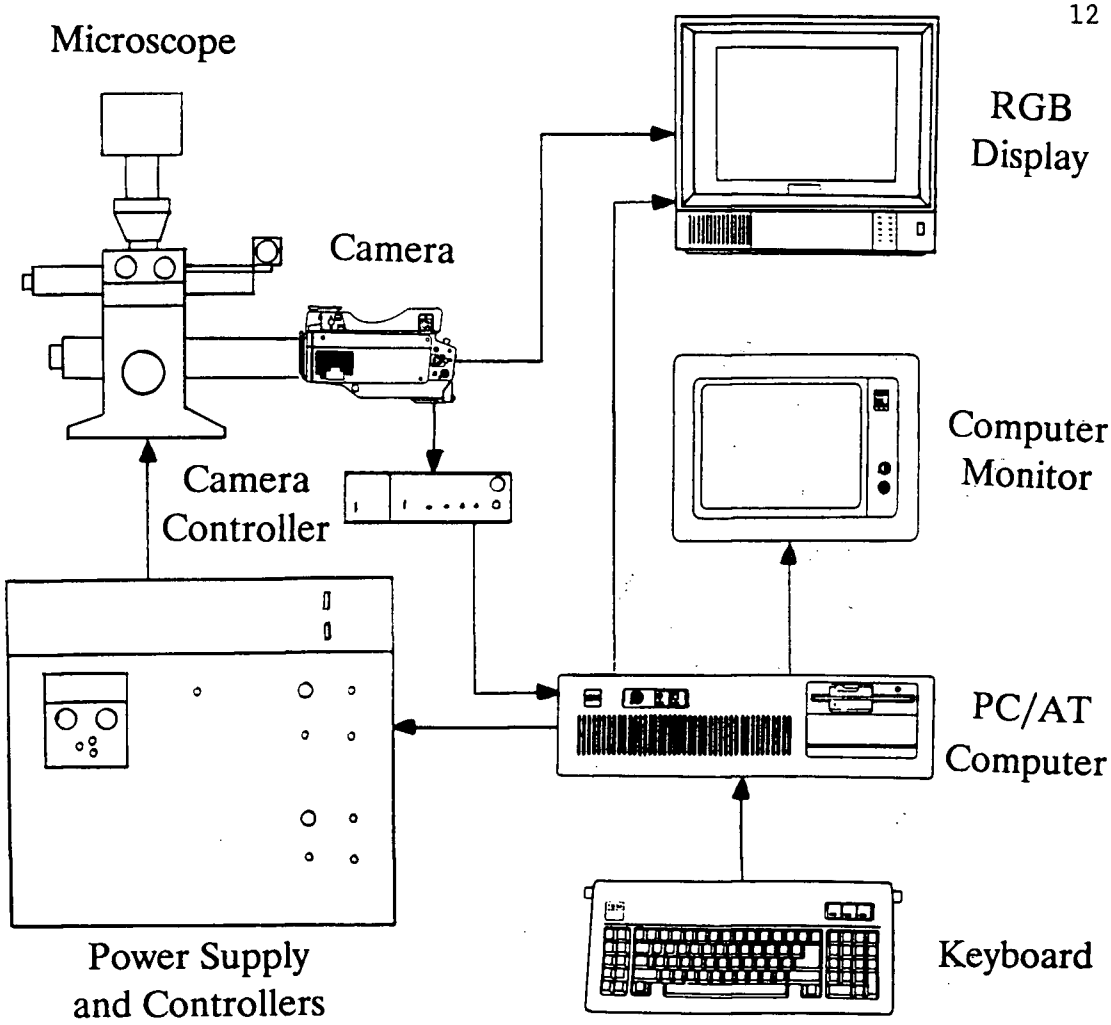

Figure 3

LAYOUT OF CELL ANALYZER IMAGE SYSTEM

The layout of the major components of the Cell Analyzer Imaging System consists of a microscope, camera, camera control unit, RGB monitor, computer, computer monitor, keyboard, and a rack containing the power supply for the light source and the controllers to move the stage in the x,y and z positions.

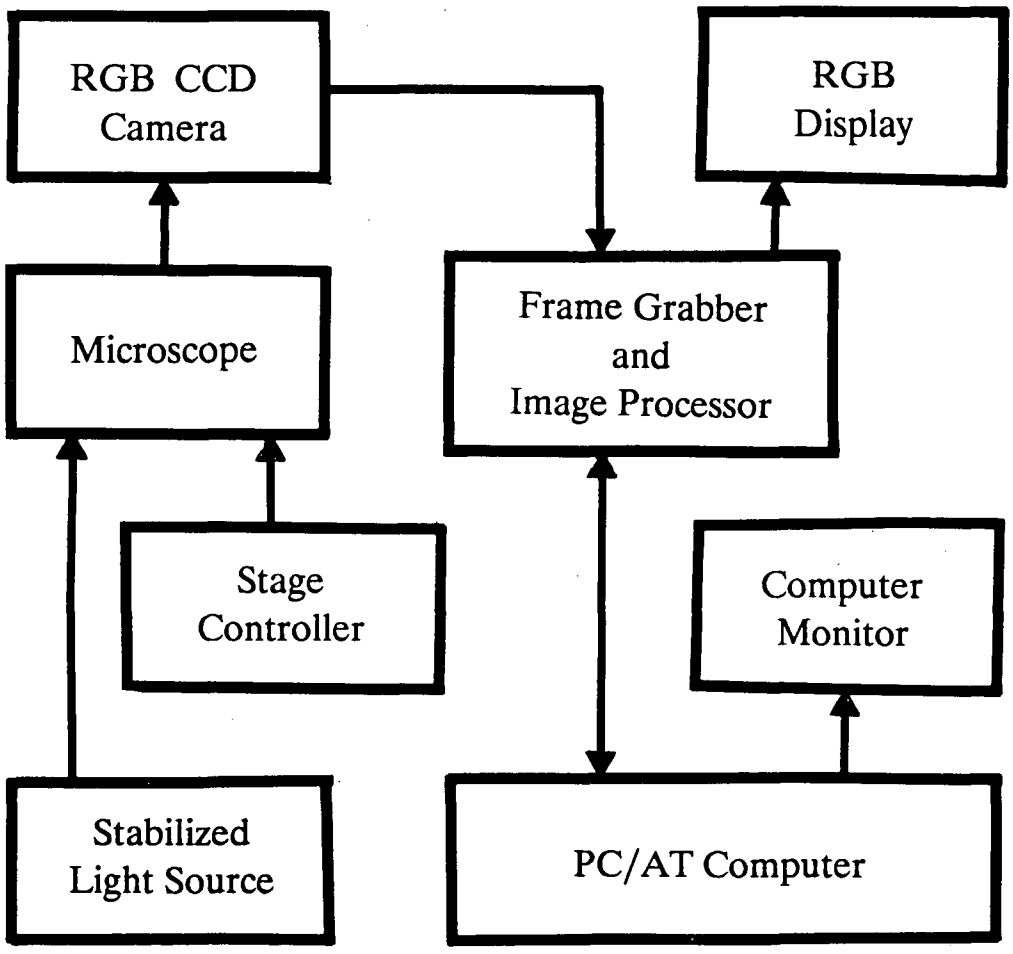

Figure 4

BLOCK DIAGRAM OF THE CELL ANALYZER IMAGING SYSTEM

The major components of the system are the stabilized light source for illuminating the sample, a stage to move the object into the microscopes field of view, the microscope optics to magnify the image, the camera to acquire the images, digitizing circuitry to transform the video signal into digital format which can be stored into image memory and displayed on an RGB monitor or manipulated by a computer.

blood and cervical cells as well as experiments of other cells and tissues which require an interactive use of an imaging system.

The Cell Analyzer system is particularly useful for developmental work. Since many stained slides contain multi-spectral information, a 3-chip CCD camera (Sony DXC-3000A) is employed to capture images in the three primary colours of the spectrums: red, green and blue. A frame grabbing and imaging board (Matrox MVP-AT) is used to digitize, store, process and display the image. This board accepts three input channels, one for each spectrum, and stores each image in one of the four 512x512x8 frame buffers. The hardware processing features of this board include histogram processor, 3x3 convolutions, and 3x3 morphological operators. Other processing and analysis functions are performed by the host IBM PC/AT computer.

For blood smear analysis, an objective lens (Plan Apochromat 40x with a 0.95 numerical aperture, air) is used in conjunction with a matched condenser lens and a TV relay lens (1x) giving a spatial resolution of 0.33 microns in both x and y directions. All three colour images of the camera are used, each of which has a photometric resolution of 8 bits or 256 grey levels.

Chapter 3
Segmentation Techniques

3.1 Overview

Many segmentation techniques have been developed over the past several decades (eg. Fu and Mui, 1981; Davis, 1975). These methods can be categorized into three different classes: i) characteristic feature thresholding or clustering, ii) edge detection, and iii) region extraction. A single algorithm generally cannot segment a particular scene and hence a combination of segmentation processes is often used. Generally these processes perform well in some applications but may fail in others. Detailed descriptions of the different classes of known segmentation algorithms are discussed in the following sections.

3.2 Thresholding or Clustering

Thresholding is a common technique used in segmenting regions in a scene. The process assigns distinct labels to areas based on some properties of the image. A property may be a characteristic feature such as the image gray levels or may be of local nature such as the gradient or Laplacian of the gray levels. In all cases, a specified range of values of a given property is used to define the pixels in the image which belong to the same region. Often, a histogram of an image property is used to determine the thresholds for each region. These

histograms are generally smoothed to remove noise. Care must be taken, however, to avoid smoothing out small but valid minima or maxima.

A thresholding technique which can be applied to gray level histograms is the mode method. This type of histogram gives an indication of the number of pixels which have the same gray level in the image (Figure 5). Thus, each peak (mode) of the histogram represents areas of similar intensity level. A boundary is placed at the valley between peaks to separate the regions. The rationale for choosing such points is to minimize the probability of misclassifying each region. Since the number of pixels at the valley compared to the peaks is relatively small, misplacement of the threshold from the exact location has relatively little effect on the resulting image. For example, Wermser, Haussmann and Liedke (1984) used this technique to segment the blood cells from the background of the image.

A different technique is used for thresholding gradient histograms. Since these histograms represent the sum of the magnitude of gradients at a given gray level, the boundary is placed at the highest point in the histogram. This point signifies the location of the largest differences (the edges) of the image. This method works well with some images but fails in others. For images where there are many similar intensity pixels with a small gradient, their sum may overmask the sum generated at the edge of rare objects and hence generate a wrong threshold level.

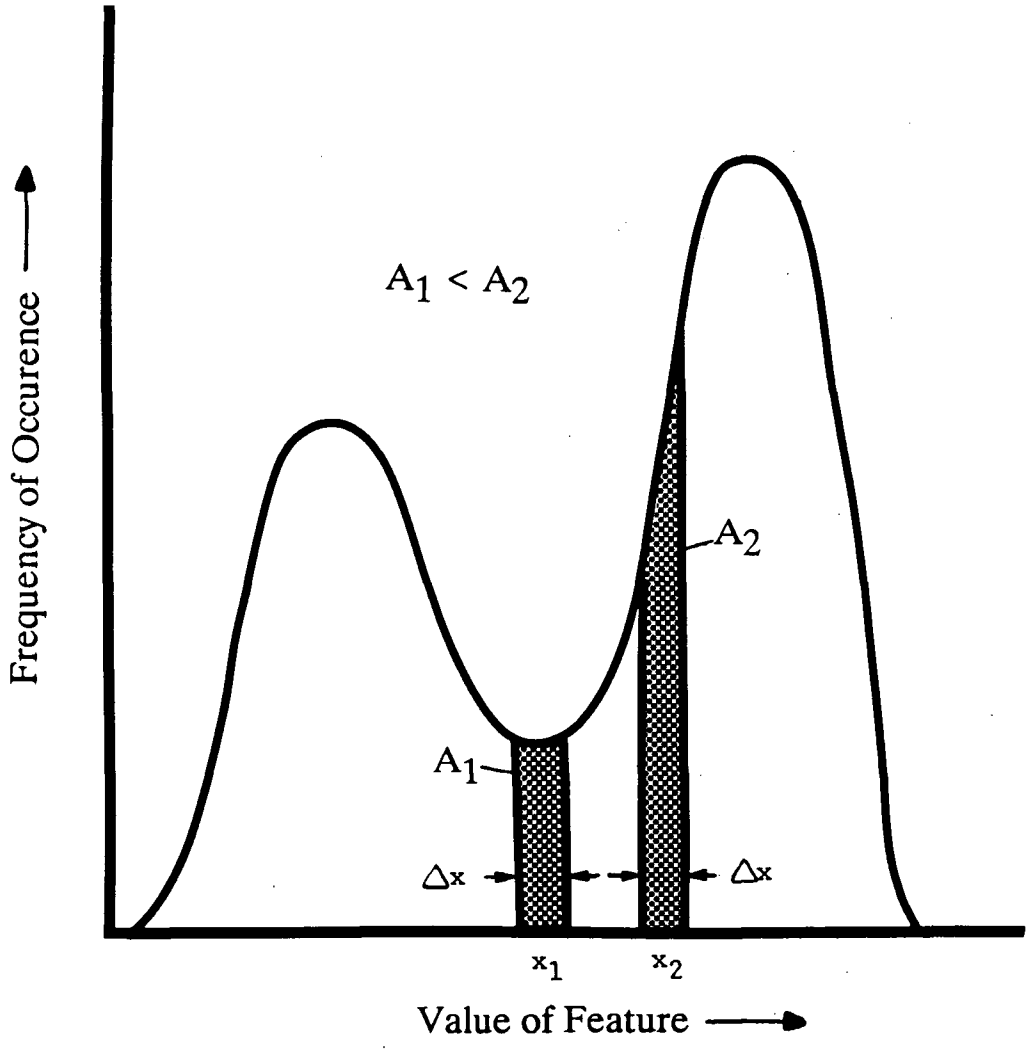

Figure 5

SELECTING A THRESHOLD IN A BI-MODAL HISTOGRAM

The threshold boundary is placed at a valley between the peaks. The error in misplacing the boundary is less at the valley (x_1) than at other points (x_2).

Clustering extends the technique of thresholding to the multi-dimensional space. This technique is used when poor discrimination exists employing a single feature but distinct regions can be detected using histograms of two or more characteristic features (Figure 6). Any feature which is useful for segmenting a region, such as the gray levels of images seen through different spectral filters, gradients, texture features, etc., can be used. Haussmann and Liedtke (1984) use the green and blue image components of the image to separate the nucleated cells from the red blood cells. Algorithms for cluster analysis have been available for locating the decision boundary between regions in a multi-dimensional space (Amadasun and King, 1988; Umesh, 1988). To reduce the amount of computations required in the analysis, the smallest number of features which can discriminate the regions is employed.

Thresholding and clustering techniques are global operators which use some aggregate properties of different features. These features are very dependent on the type of regions which are segmented in the image. Although the segmented regions are closed, some images may require smoothing to eliminate the noisy boundaries. Since no spatial information is used in the selection of the threshold, the resulting regions may not be contiguous.

3.3 Edge Detection

Edge detection algorithms use the information of edge points to determine the boundary between objects. The edge points are located

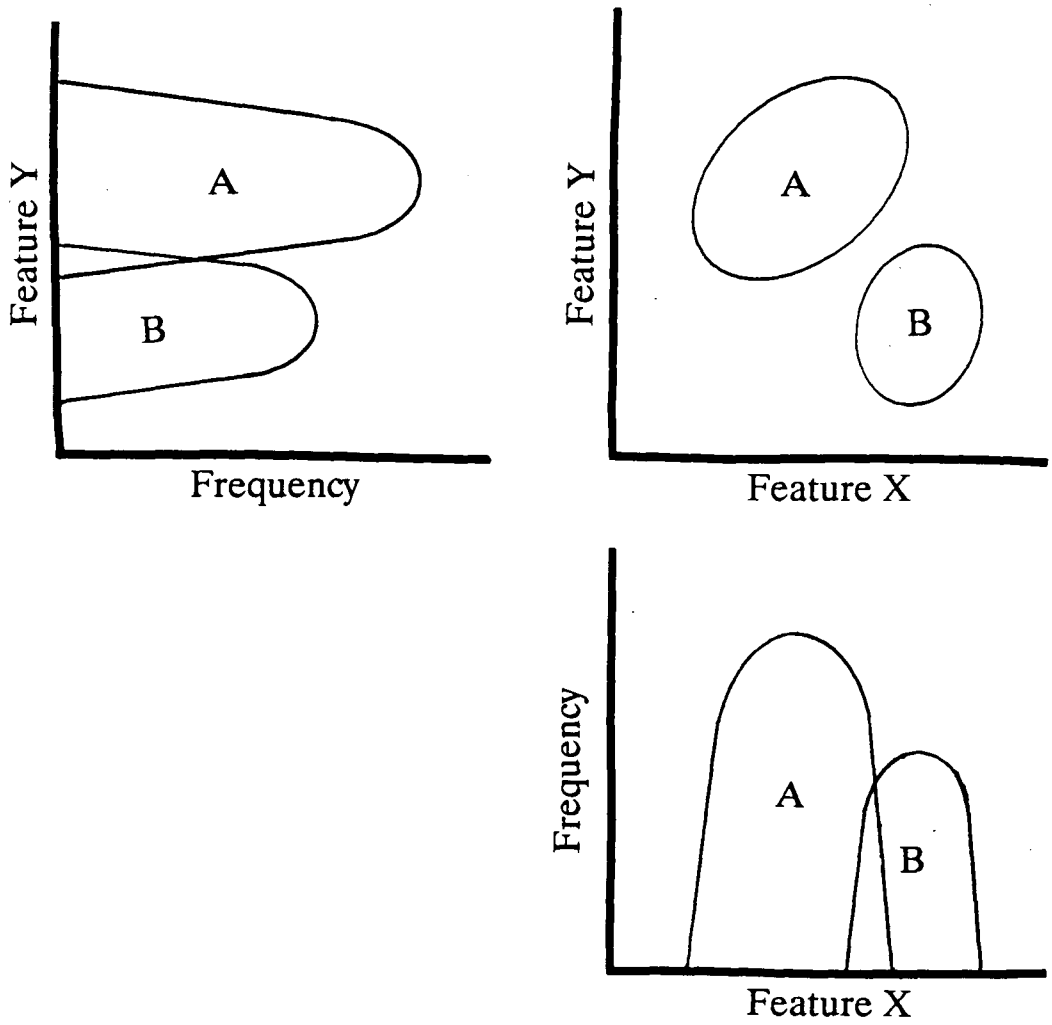

Figure 6

USE OF CLUSTERING IN OBJECT DISCRIMINATION

Objects in group A can be easily separated from those in group B in the two-dimensional (x,y) feature plot. This is not the case in either of the one-dimensional feature plots.

where there is an abrupt change in gray levels in the image. In this technique, the elements which are candidates to belong to an edge are first extracted and then combined to form the boundary.

The extraction of edge pixels requires a measure which corresponds to the change in gray value of the pixel with its surrounding. Various methods, such as the gradient, Sobel, Kirsch, and Prewitt operators (Rosenfeld and Kak, 1982; Young and Fu, 1986), have been developed for this purpose. These operators can be implemented as a series of image convolutions where the weights in the convolution kernel is different for each filter. The resulting value gives an indication of the strength of the changes around each pixel. The edge points are then extracted by thresholding the processed image. Marr (1982) has developed a Laplacian of a Gaussian edge filter. In this method, the zero-crossings of the filter correspond to the edges of the structures which have a space constant greater than (or a lower spatial frequency than) a selected value used in the Gaussian blurring process.

There are several problems with edge detection techniques. This is because the transition from one region of the image to the other sometimes occurs over several pixels and is then not abrupt enough. The contours produced from thresholding edge information are generally more than one pixel wide and not necessarily closed. Hence, some post-processing using thinning and contour-closing algorithm is required. Another problem is that the texture of some regions are significant enough to be thresholded as edge points resulting in erroneous image

segmentation. Nevertheless, the results from the edge detection techniques can be used in conjunction with other methods in determining particular regions.

3.4 Region Extraction

Another approach to segmentation is to group pixels with similar properties, such as gray levels, texture, color information, etc., into regions. These region extraction techniques can be separated into three categories: region merging, region splitting, and a combination of region merging and splitting.

In region merging or growing techniques, the image is initially divided into many small regions such as a pixel or a small neighbourhood of pixels. Various properties that reflect the characteristics of the object are computed for each region. The characteristics of each region are compared with its neighbouring regions. If the properties of the adjacent regions are similar, these regions are combined or merged into one. This process is iterated by recomputing the object membership properties for each enlarged region and merging the regions which have similar characteristics. The segmentation is completed when all adjacent regions have significantly different properties such that no merge can further be made.

The region splitting or dividing techniques begin with the entire image instead of many small regions. A predicate describing the various

properties of the object is evaluated from the entire region. An example is to determine if all pixels in the region have gray levels which do not differ by a certain amount. If the predicate is not satisfied, the region is divided into smaller regions and the predicate for each of the sub-regions is recomputed. The process continues until the predicates for all regions are satisfied.

The split and merge technique uses a combination of region merging and splitting to obtain regions of similar properties. Regions are merged when adjacent regions have similar properties and are split when the predicate describing the property is not satisfied. Liedtke et al. (1987) used this technique on blood cells to extract the primitives used in his segmentation method.

Region extraction techniques utilize the local properties of the image directly. Although they produce closed and contiguous regions, the drawback is that these algorithms are computationally intensive.

Chapter 4
Blood Cell Analysis Algorithms

4.1 Overview

A program was designed and written to incorporate the algorithms which are developed to automatically segment nucleated blood cells. The approach for analyzing these cells involves the following seven steps: i) acquisition of images, ii) pre-processing the acquired images, iii) detection of possible cells in the scene, iv) segmentation of the cells in the scene, v) post-processing the segmented regions, vi) extraction of features, and vii) classification of the object (Figure 7). The first two steps, acquiring and pre-processing the images, are critical since high quality input images will simplify and reduce the amount of processing required in the later stages of the analysis. The manipulation of spectral information is used in the following step to detect the cells in the scene. All nucleated cells are selected from the background and non-nucleated red blood cells. Once the cell locations are found, all single cells are accounted for and also any cells which are just touching are separated and the boundary of each isolated cell is determined. The next step is to segment the isolated cells into two regions: nucleus and cytoplasm. Post-processing of the defined regions is required to fine-tune the mask of each region. Features are then calculated based on the defined region boundaries. The cells in the scene are then classified based on the values of the features.

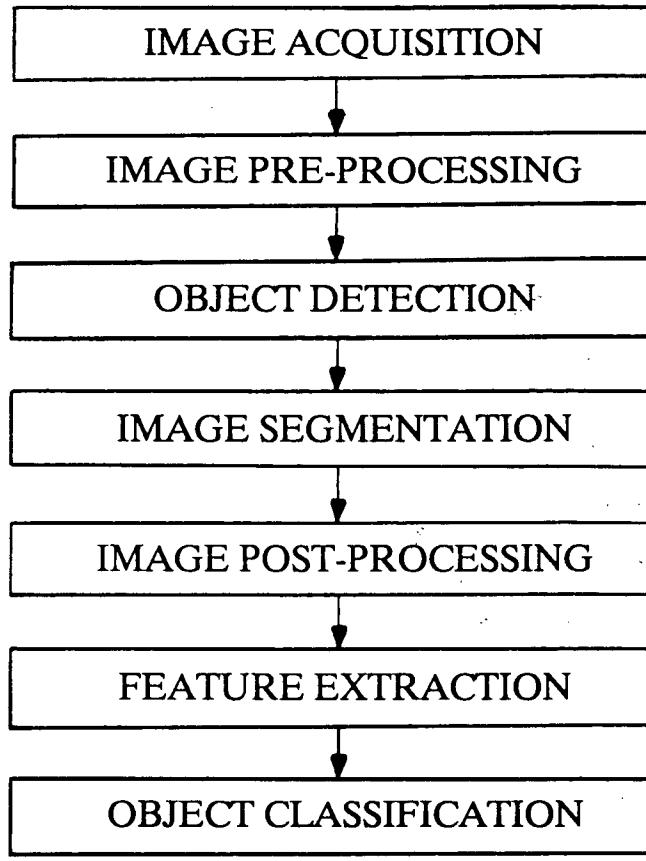

Figure 7

BLOCK DIAGRAM OF THE PROCEDURES TO ANALYZE BLOOD CELLS

Algorithms are employed in the acquisition and pre-processing sections to ensure that the images used in the analysis are corrected for. Errors in the detection and segmentation sections should be minimized to limit their propagation to the later parts of the analysis. Features are extracted from the segmented regions and the classification of the object is made based on the feature values.

The most difficult portion of the analysis is to define the regions of the cell. Unlike feature extraction where only mathematical algorithms will suffice, segmentation also requires prior knowledge of the geometrical, morphological, and topological properties of the cells in the scene as well as a heuristic approach for analyzing the problem. Since object classification is based on feature values which are derived from the segmented regions, the segmentation is crucial for the correct interpretation of the cells in the scene.

4.2 Image Acquisition

Since each region of the blood cell is stained a different colour and multi-spectral analysis is used, two or more images taken with different colour filters must be obtained.

Camera calibration must be performed at the beginning of each experiment to ensure correct colour registration of the image. This is accomplished by adjusting the gain and offset of the amplifiers for each colour component (red, green and blue) such that a similar light level is observed at the output of each channel when only the background light is measured.

Light source and frame grabber calibration is also executed before the experiment begins. In order to utilize the full photometric range of the digitizer (8 bits or 256 grey levels), the voltage level of the light source and the gain and offset of the analogue to digital

converter of the frame grabber board are adjusted accordingly. The level of the background, which is the brightest part of the image, is set to approximately five percent below the maximum to avoid image saturation. The darkest stained nucleus in the image is set to approximately five percent above the minimum detectable level.

In the analysis, images from each of the red, green, and blue colour spectrum are acquired. Since the scene is static, an average of a number of images from each spectrum is taken beforehand. This averaging has the effect of reducing the random noise introduced by the light source, detector and digitizer. Since each detected image $I_i(x,y)$, can be represented as a sum of a stationary part $S(x,y)$, and a part containing random noise $N_i(x,y)$, i.e.

$$I_i(x,y) = S(x,y) + N_i(x,y) \tag{1}$$

the average of M images is of the form

$$I_{av}(x,y) = \frac{1}{M} \sum_{i=1}^{M} \{S(x,y) + N_i(x,y)\}. \tag{2}$$

If the noise is assumed to be uncorrelated with the image, then it can be shown that the power spectrum of the noise (S_{NN}), is reduced by a factor of M (Castleman, 1979; Pratt, 1979), i.e.

$$(S_{NN})_{av} = \frac{1}{M} (S_{NN}) \tag{3}$$

where $(S_{NN})_{av}$ is the power spectrum of the noise in the averaged image. If the noise is assumed to have a Gaussian distribution, then the standard deviation σ, of the random noise is reduced by the square root of the number of frames averaged, i.e.

$$\sigma_{av} = \frac{1}{\sqrt{M}} \sigma_i \tag{4}$$

where σ_{av} is the standard deviation of the noise in the averaged image. Due to the quantization limit, the standard deviation of the averaged image is chosen to be at most a half of a grey level ($\sigma_{av} \leq 0.5$). Achieving this average noise level implies that the number of frames required for each sample (i.e. the number of frames to be averaged) should at least be four times the variance of the detected random noise, i.e.

$$M \geq 4 \sigma_i^2 \tag{5}$$

The standard deviation of the grey level of the random noise in the acquired spectral images ranges from 2 to 3. Hence, M, the number of frames averaged for each image analyzed, is chosen to be 36 (Figure 8).

4.3 Image Calibration

Although random noise can be reduced by averaging, fixed pattern noise must be corrected by using other means. These noise patterns are

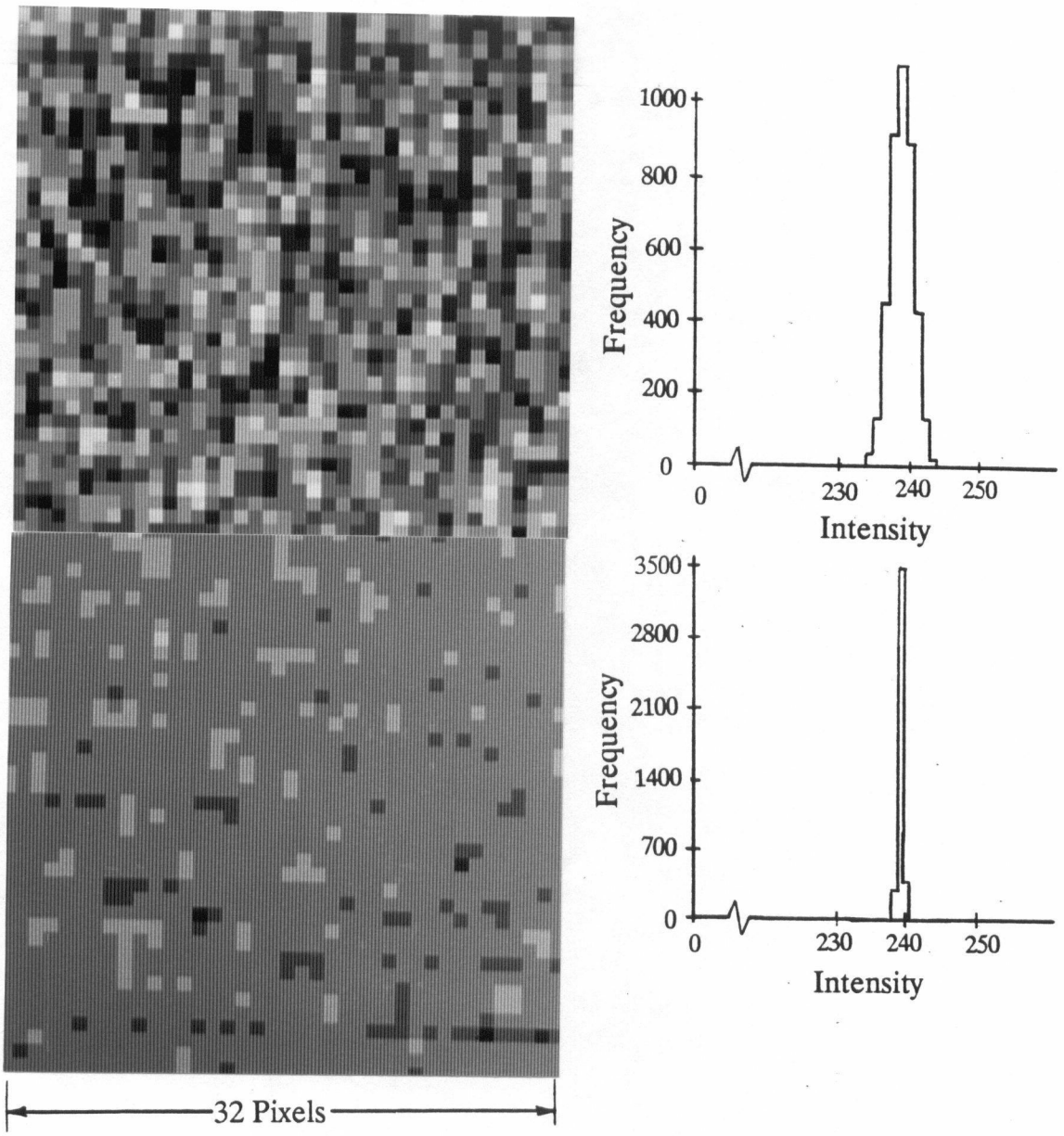

Figure 8

NOISE REDUCTION DUE TO IMAGE AVERAGING

The variation in background intensity in the original image and its histogram (top) can readily be seen. The color mapping table is adjusted to highlight small changes in intensity levels. The same image was captured 36 times and averaged (bottom) to reduce the noise variations.

produced by various components in the imaging system. Unequal sensitivity between elements of the detector results in different gray level values among pixels that have received the same illumination. Some camera control circuitries generate evenly spaced vertical bars with slightly varying intensities. Shading and aberration effects caused by the optics also produce uneven illumination at the detector resulting in a brighter spot near the centre of the image which fades to the edges.

Decalibration is one method which is used to correct the fixed pattern noise. Each pixel in the image I(x,y) is transformed into a new image C(x,y), using an equation involving the bright background image B(x,y), a dark image D(x,y), and a constant scaling factor k:

$$C(x,y) = k \frac{I(x,y) - D(x,y)}{B(x,y) - D(x,y)} \qquad (6)$$

This formula represents the transmittance of the image where each pixel is corrected for by the values of the calibration images. A range of bright and dark images is used to linearly map the detected image to a scale of 0 to k. Because division is used, truncation error is likely to distort the distribution of gray levels. In bright field microscopy, the dark image usually has a gray level of 0 and the bright image has a intensity ranging from 200 to 220. Hence, up to 10% improvement is seen using the decalibrated instead of the raw image.

Background subtraction of optical densities can be used instead to achieve a similar result. This method is based on the conversion of the transmittance to optical density by taking logarithm of the pixel values; the dark image is assumed to be zero in this case.

$$\log C(x,y) = \log I(x,y) - \log B(x,y) + K \tag{7}$$

where the background is subtracted from the original optical image and a constant value of K is added to offset the intensity distribution. Taking logarithms on a discrete image will produce gaps in the distribution of the optical density profile which adds complications later in the analysis of the images.

A third approach to correct images is to subtract the bright image and then add an offset equal to an average value of the bright image, i.e.

$$C(x,y) = I(x,y) - B(x,y) + K. \tag{8}$$

This approach was used to analyze white blood cells in this work (Figure 9). The method adjusts each pixel by adding an offset such that a bright background image appears to have equal gray level value for all pixels. Most of the image consisting of background pixels is correctly adjusted for. The advantage of this method is that no truncation error is introduced since only subtraction of integers is involved. Although the approach is not as good as the first two methods, it does serve as a good approximation for image correction. The error in the correction

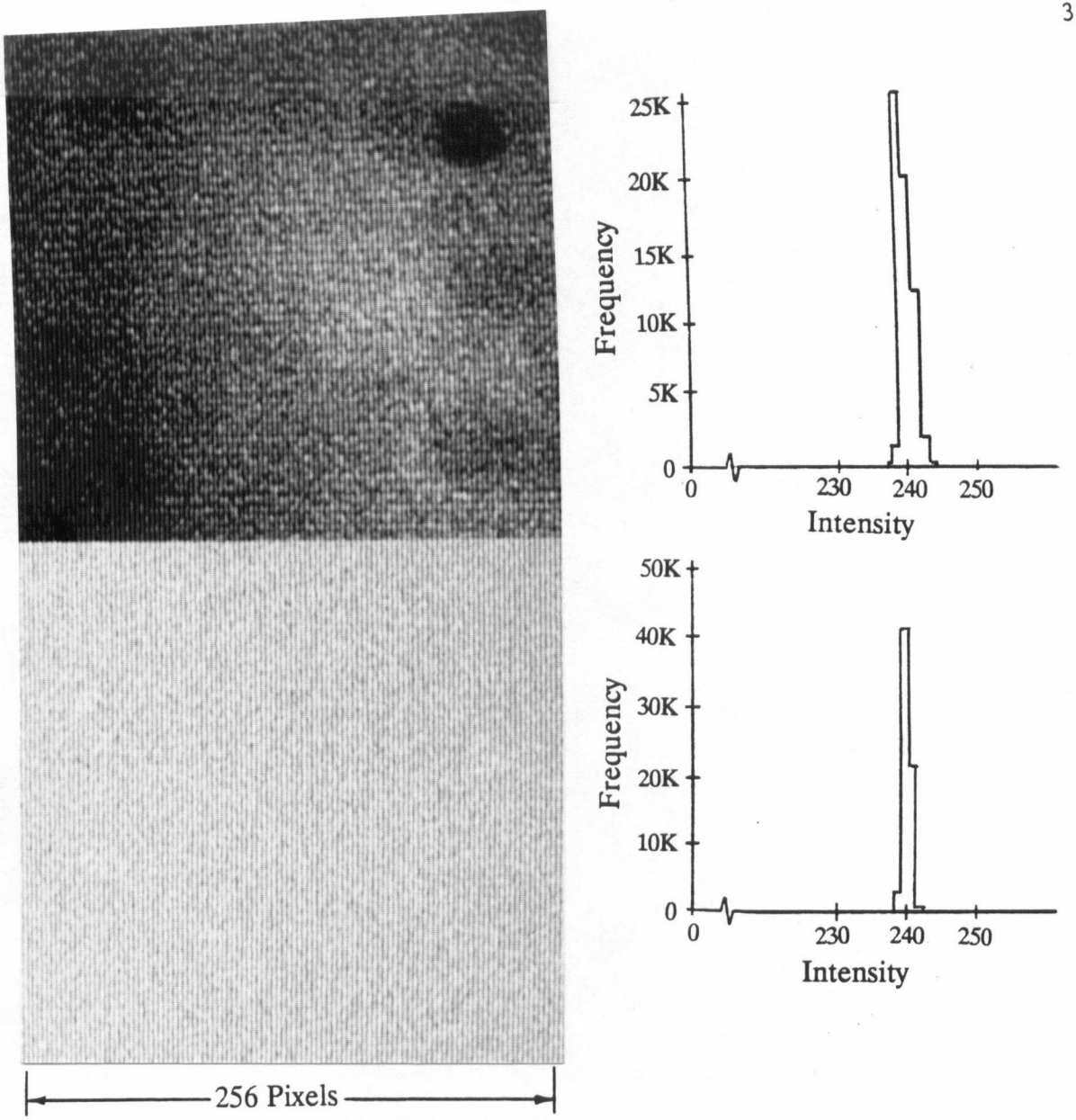

Figure 9

NOISE REDUCTION USING BACKGROUND SUBRACTION

The aberration and shading effects in the original image and its histogram (top) can readily be seen. The color mapping table is adjusted to highlight small changes in the intensity levels. Background subtraction (the third method as described in the text) was then applied to the image (bottom) to remove this shading effect.

does increase in the darker regions where the stained cells lie, but the change in the error is gradual and insignificant in affecting the segmentation algorithms.

4.4 Recognition of Nucleated Cell

The first step in the analysis is to determine if there are any nucleated cells of interest in the image. Since colour is used for visual detection of nucleated cells, red, green, and blue spectral information was used. To illustrate this point, two colour histograms with colour information on each of its two axis, and the frequency of occurrence of a particular colour pair on the third axis was generated as shown in Figure 10. It can be seen that no single threshold can be used in any of the individual colour histograms to separate the nucleated cells from the rest of the image. However, the regions of the nucleus and the cytoplasm of the nucleated cells, the red blood cells, and the background form clusters in the two colour histograms.

Wermser, Haussmann and Liedke (1984) proposed a method for analysis of a one dimensional histogram on Pappenheim stained peripheral blood smears instead of the more time consuming multidimensional cluster analysis. In this approach, characteristic feature X(x,y), is generated from a linear combination of the green G(x,y), and blue B(x,y), images:

$$X(x,y) = a\ G(x,y) + b\ B(x,y) \qquad (9)$$

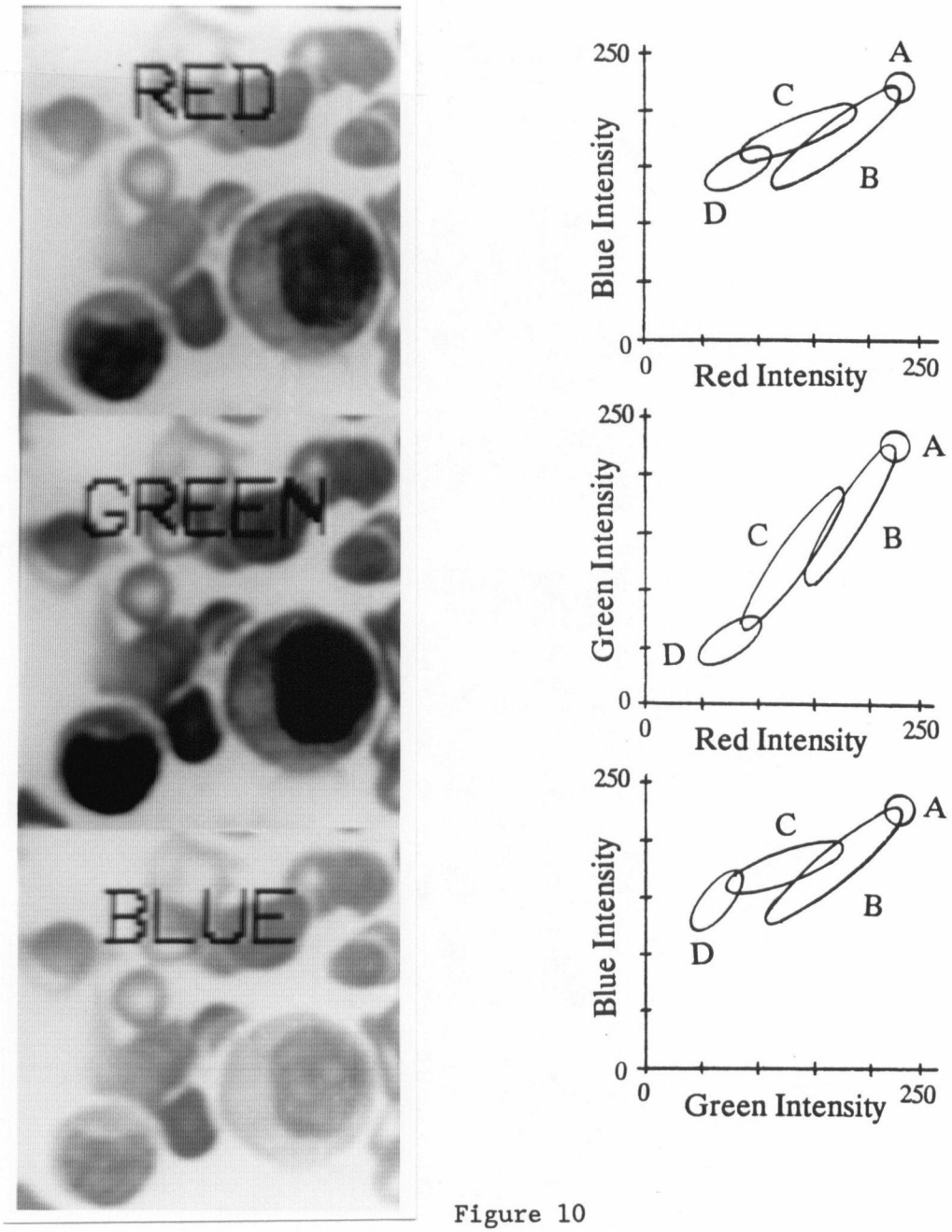

Figure 10

CLUSTER PLOTS OF SPECTRAL IMAGES OF BLOOD CELLS

A photograph of the intensity variations of each of the spectral images (left): red, green, and blue (from top to bottom), and cluster plots of each of the two colours (right): red-blue, red-green, and green-blue (from top to bottom), are shown. Clustering of the (A) background, (B) red blood cells, (C) cytoplasm, and (D) nucleus areas can be seen.

where a and b are constants using values of a=0.390 and b=0.546. A histogram of the new image is generated and a simple threshold at the valley of the histogram of this characteristic feature is used to separate the red blood cells from the cytoplasm of nucleated cells.

A similar approach can be employed with the Wright's stained cells used in this work. The characteristic feature uses the red, R(x,y), and blue, B(x,y), images in a formula:

$$X(x,y) = R(x,y) - B(x,y) + 128 \qquad (10)$$

This method involves simple subtraction of the images. No floating point arithmetic is involved which would introduce truncation errors. The constant value of 128 is added to shift the origin such that values from -128 to 127 are mapped to the values 0 to 255.

To extract the nucleated cells in the image, thresholding on the histogram of the smoothed subtracted image is performed. The subtracted image is first averaged to remove speckled noise at the edges of the red blood cells. This filter consists of convoluting the image with a 3x3 kernel of weights equal to 1's and dividing the result by a factor of 9. A histogram of this filtered image is produced (Figure 11). The threshold T, near the valley is found by selecting the first point to the left of the peak where pixels belonging to the red blood cells and background are represented in the histogram H(T), and which has a gradient less than 2% of the maximum peak value P_{max}, i.e.

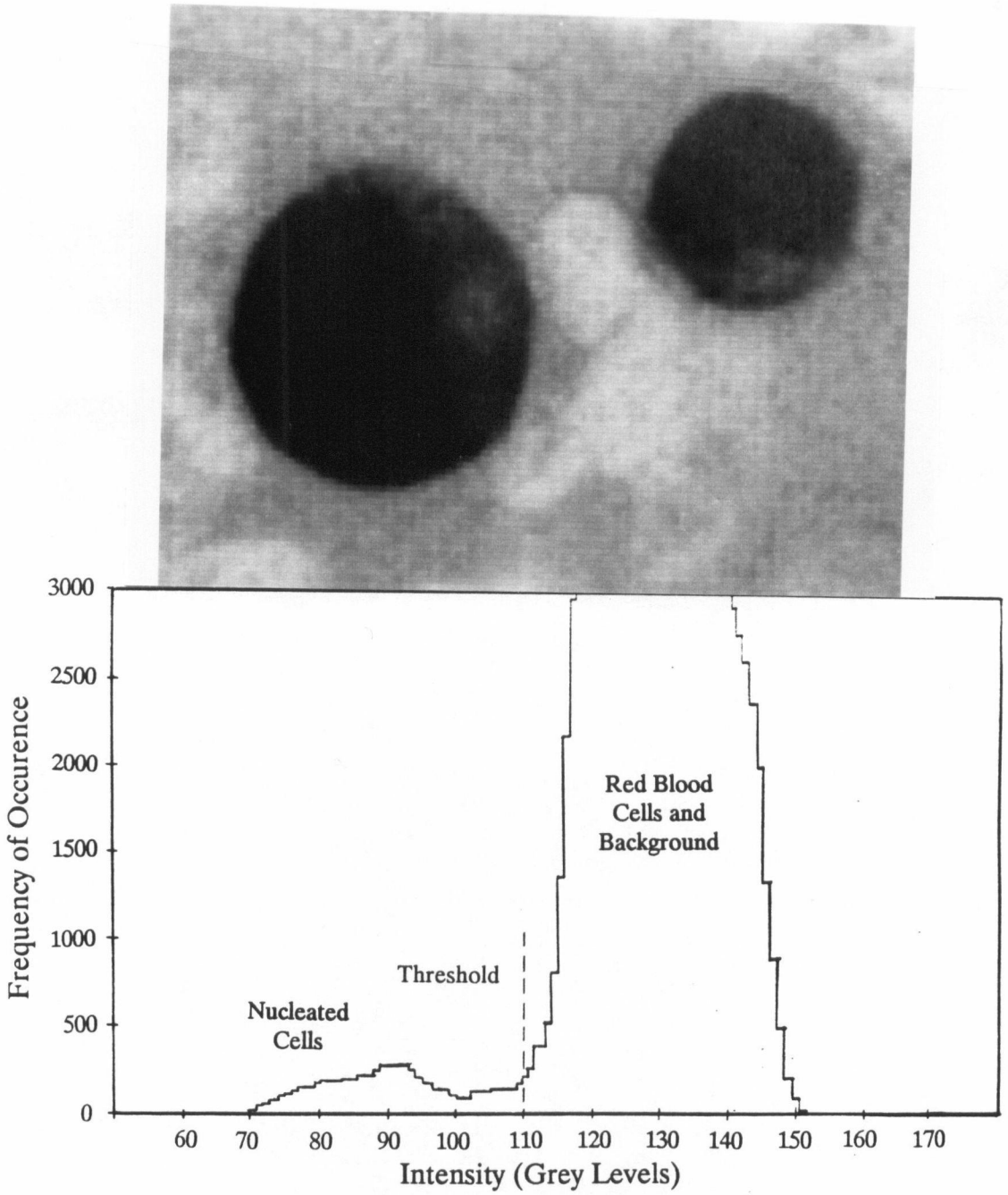

Figure 11

SEGMENTATION OF NUCLEATED CELLS

The photograph of the blue image subtracted from the red image is shown at the top. Because of the noise in the image, a filtered version of the image histogram is used to determine the location of the threshold (bottom).

$$H(T) - H(T-1) < 2\% \; P_{max} \qquad (11)$$

All pixels below this threshold are set to a gray level of 255 (the cell mask) and all other pixels are set to 0. The 2% P_{max} gradient threshold is selected experimentally to optimally encompass not only the nucleated cells but also several pixels belonging to the red blood cells. If a higher gradient threshold is selected (greater than 2% P_{max}), more red blood cells will be included in the cell mask. If a lower gradient value is chosen, some of cytoplasm of the nucleated cells will be lost to the background region. A 3x3 median filter is applied on the cell mask to fill the holes in the white blood cells and to remove the unwanted points in the red blood cells and background. This filter acts as a low pass filter removing any high spatial frequencies from the image. Because a binary image is used as the input, the filter can be implemented as a local 3x3 average operation on each pixel and then the result is thresholded at the 128 level to generate the new binary mask. A single dilation followed by two erosions using a 3x3 window are applied to this binary image to fill the larger holes and smooth the contour of the nucleated cell mask (Figure 12). In the dilation process, a pixel is included in the new cell mask if any of its eight adjacent neighbours belong in the cell mask. In the erosion process, a pixel is removed from the cell mask if any of its eight adjacent neighbours does not belong to the mask.

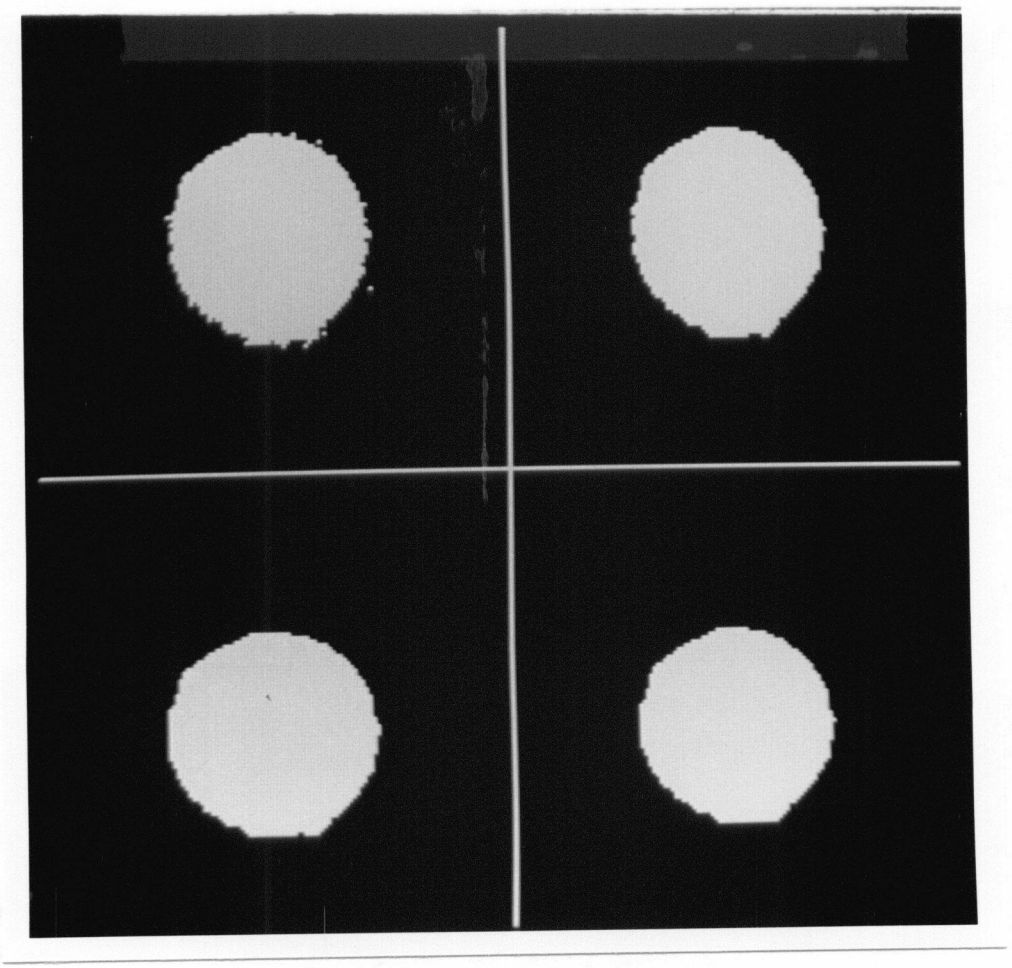

Figure 12

SMOOTHING THE NUCLEATED CELL MASK

The process of the operations used to smooth the nucleated cell mask is shown. The original nucleated cell mask is shown in the top left. A low pass filter is first applied to the mask (top right), followed by a dilation (bottom left) and two erosions (bottom right). Jagged edges are smoothed, holes are filled, and small fragments are removed by these processes.

4.5 Boundary Detection of Single Cells

Some of the nucleated cells extracted from the mask may be useful for further analysis. Because of the complexity and the high error rate in segmentation, certain arrangements of cells can not be analyzed. These include overlapping nucleated cells or cells which are too close together that even a human observer would have a hard time segmenting them properly. Hence, only nucleated cells which are standing alone or are just touching were used for further analysis.

To extract these cells, the nucleated cell mask is searched until the boundary of a cell is encountered. A boundary chain code starting at this point is then generated. The chain code is a boundary numbering scheme that labels each boundary point with the direction code (Figure 13) of one of its eight possible neighbours as the next boundary point. Hence, a consecutive list of these points defines the boundary of the object.

3	2	1
4	centre	0
5	6	7

Figure 13

BOUNDARY DIRECTION CODES.

This coding scheme is used to label the boundary points of the next point relative to the centre location in the boundary chain code.

An algorithm has been developed to separate touching cells based on this boundary information. The location of the boundary pixels can be calculated from the boundary chain code. This information is used to find the angle of the tangent line to each point on the object boundary. The least square fit is used to determine the slope of the tangent line based on the nine points centered at the point of interest, i.e.

$$dx(i) = \sum_{j=0}^{8} [x(j+i-4) - x(i-4)] \tag{12}$$

$$dy(i) = \sum_{j=0}^{8} [y(j+i-4) - y(i-4)] \tag{13}$$

where dx(i) and dy(i) are the total variations over the nine points in the x and y directions respectively. The angle of this line $\theta(i)$, relative to the x-axis is then calculated, i.e.

$$\theta(i) = \arctan \frac{dy(i)}{dx(i)} \tag{14}$$

By taking the difference of angles $d\theta(i)$, between points which are four boundary points away, i.e.

$$d\theta(i) = \theta(i-2) - \theta(i+2) \tag{15}$$

a noticeable peak is seen at the corresponding location of where the two cells touch (Figure 14). A value of 2π is added or subtracted from the difference angle to ensure that the result is within $-\pi$ and π.

A line segment is produced by joining the peaks to separate the touching cells. The values of this line are set to the background mask level of zero, thus separating the two cells. A smoothing operation is applied to each of the separated object to smooth any corners introduced by the separation of the touching cells.

After the touching cells are separated, all objects (cells) which are within a prescribed size are used for further analysis. This eliminates the unnecessary need to analyze objects which are too small or too large to truly represent a cell.

4.6 Nucleus and Cytoplasm Segmentation

The next step in the segmentation process is to determine the different regions of a nucleated cell: the nucleus and the cytoplasm. The mask of each single cell is overlaid on the green spectral image using the logical AND function of the mask with the image. A histogram of this masked image is generated. This histogram is generally very noisy and has more than two distinct peaks (Figure 15). Hence, an additional operation utilizing the edge information is performed to help define each region more readily and to smooth the intensity level variations in each region.

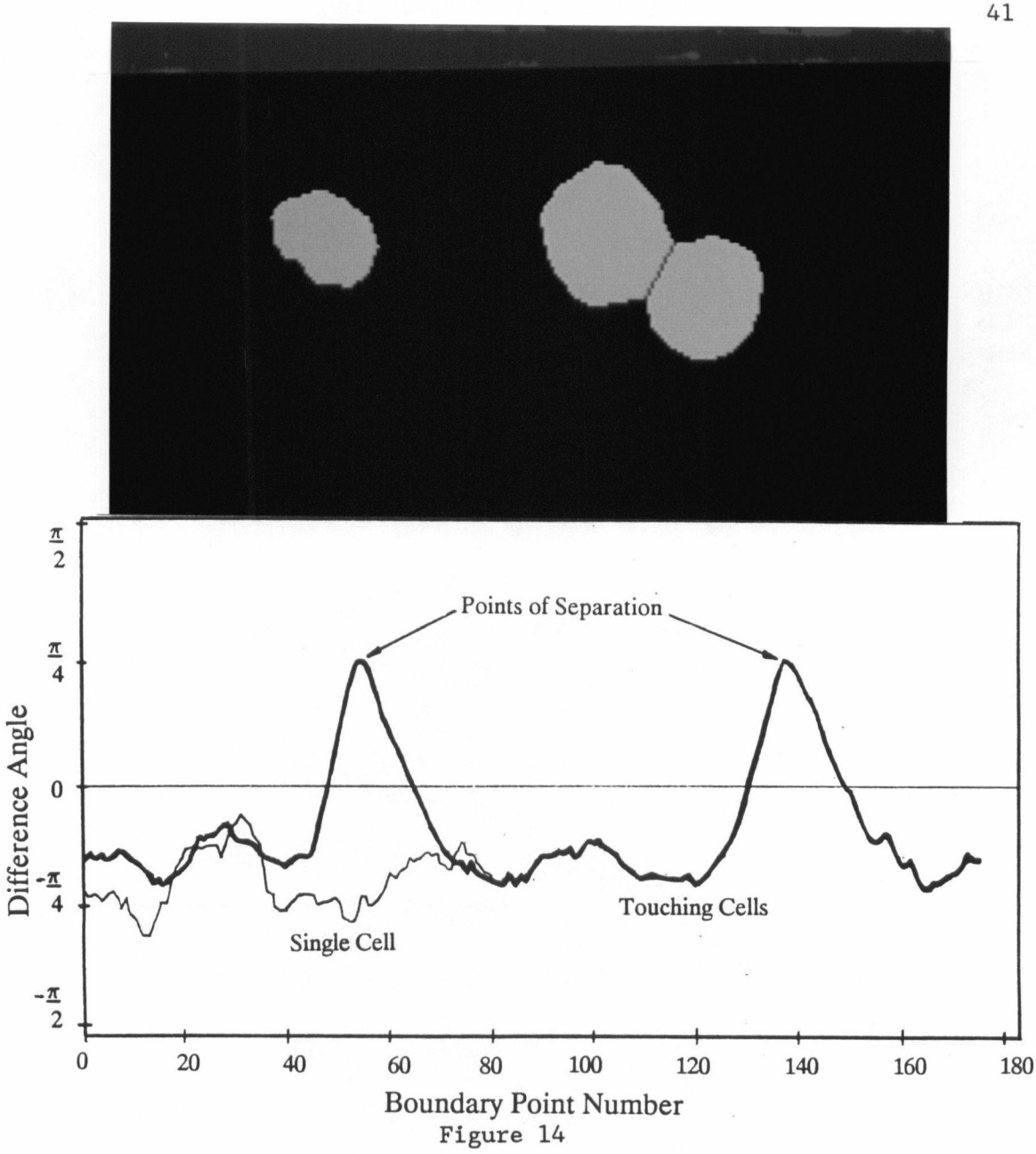

Figure 14

SEPARATION OF TOUCHING CELLS

The outline of a single and two touching cells (top) are shown. The plots of the difference of the angles of the tangent along the boundary of the single cell and the two touching cells (bottom) are shown. The two peaks in the angle difference plot correspond to the indentations found at the boundary of the two touching cells.

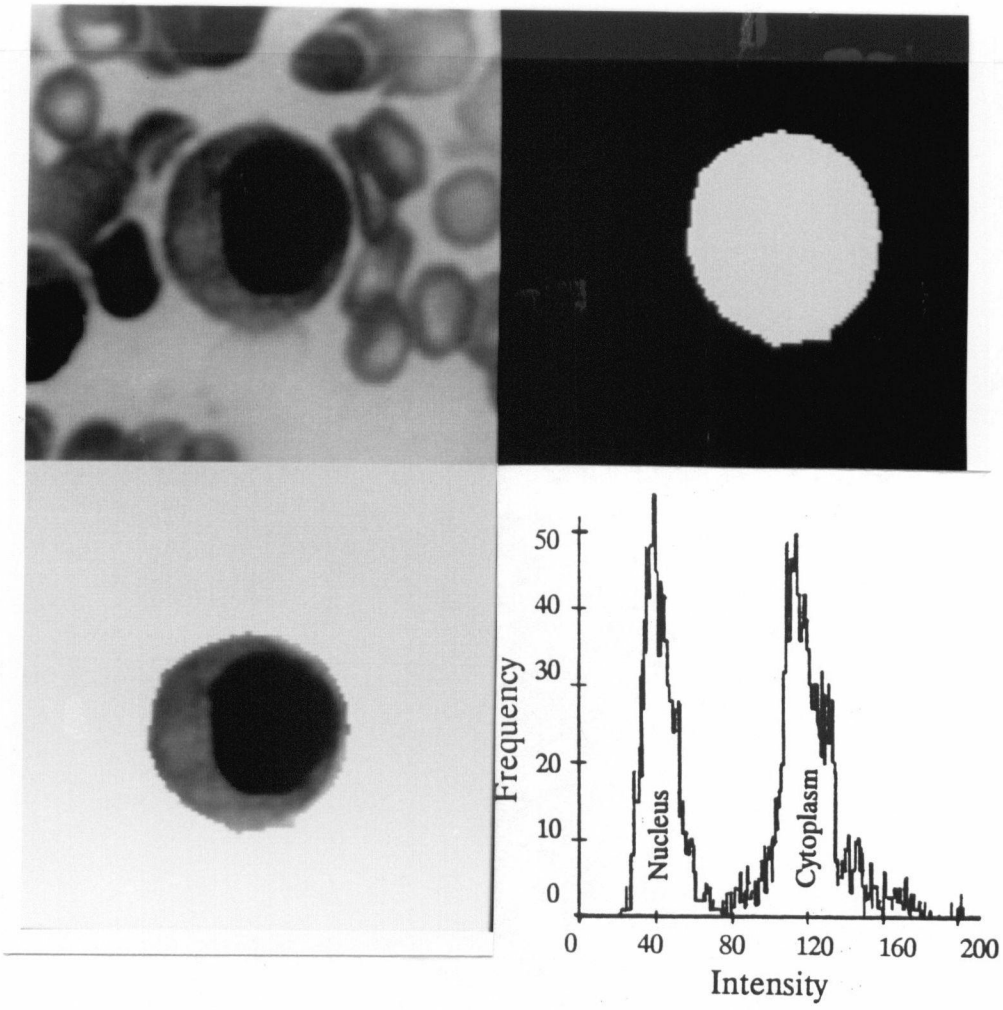

Figure 15

HISTOGRAM OF THE SEGMENTED NUCLEATED CELLS

The original image in the green spectrum (top left) and the nucleated cell mask (top left) are shown. The mask is overlaid on the original image (bottom right) to show only the nucleated cell. The histogram of the green image is generated (bottom right).

This additional operation is the conditional mean filter. In this filter, the sample mean M(P), and the sample variance Var(P), of the gray levels in a local 3x3 window at each pixel P(x,y), are calculated.

$$M(P(x,y)) = \frac{1}{9} \sum_{i=-1}^{1} \sum_{j=-1}^{1} P(x+i, y+j) \tag{16}$$

$$Var(P(x,y)) = \frac{1}{9} \sum_{i=-1}^{1} \sum_{j=-1}^{1} \{P(x+i, y+j) - M(P(x,y))\}^2 \tag{17}$$

If the variance is below a pre-defined "conditional" limit, the pixel value is replaced by the mean value. Otherwise, the value of the pixel is examined and adjusted. If the value is greater than or equal to the mean then it is replaced by the sum of the mean and standard deviation. Otherwise, it is replaced by the difference of the mean and standard deviation.

The histogram of the resulting image is used to determine the boundary between the nucleus and the cytoplasm (Figure 16). This histogram H(T), is smoothed by a 9x1 median filter to remove noisy spikes. The point T, to the right of the first dark peak where the gradient is less than 5% of the maximum peak P_{max}, is chosen as the threshold level, i.e.

$$H(T) - H(T+1) < 5\% \; P_{max} \tag{18}$$

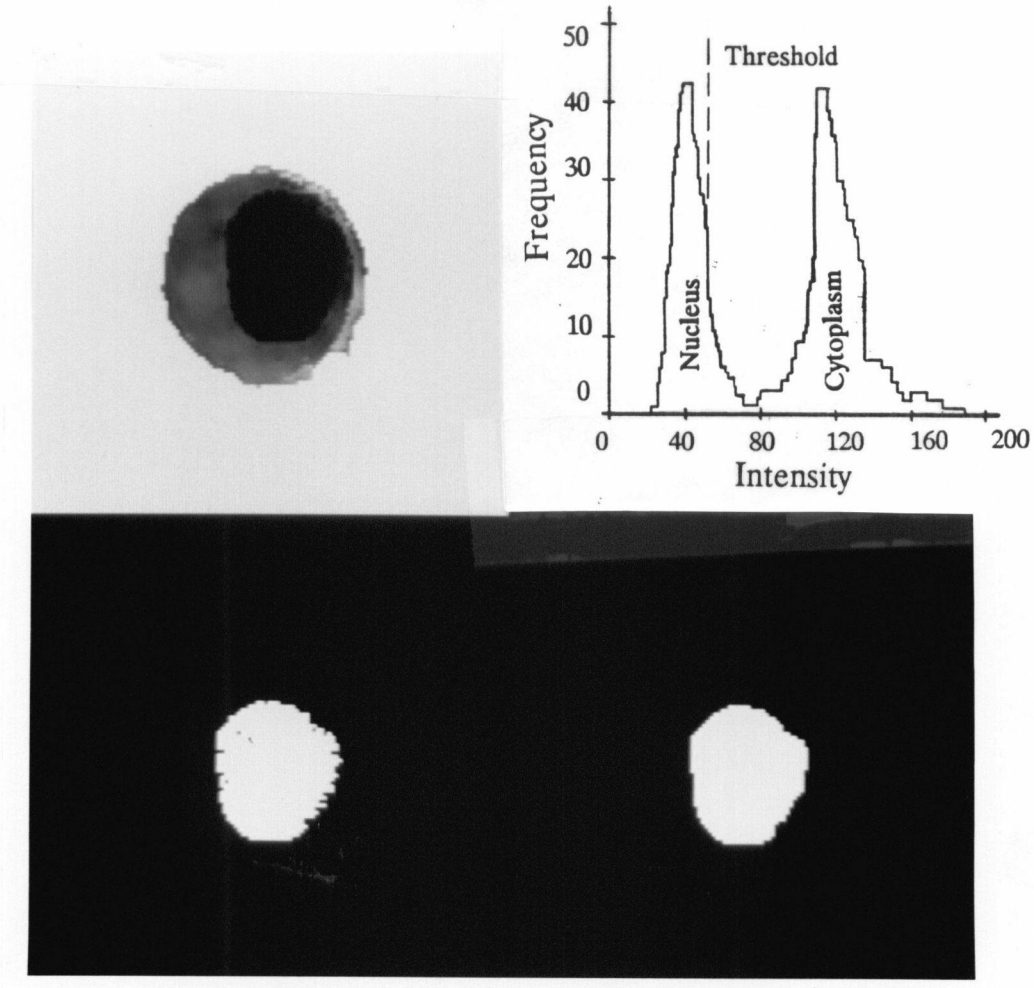

Figure 16

PROCESS TO SEGMENT NUCLEUS AND CYTOPLASM

A filter is applied to the masked image (top left) and its histogram is generated (top right). A threshold is determined on the histogram and the resulting nucleus mask is formed (bottom left). This mask is then smoothed (bottom right).

The gradient threshold of 5% P_{max} is experimentally chosen to be the optimal for generating the cytoplasm and nuclear mask. If the threshold is greater, the less dense (lighter stained parts) of the nucleus will be classified as cytoplasm. If the threshold is lower, the more dense (darker stained parts) of the cytoplasm will be included in the cytoplasm mask. A median filter and dilation and erosion operations are performed on the resulting mask to fill the holes and smooth the boundary of the nuclear mask.

4.7 Simple Feature Extraction

Features can be extracted from the regions once their boundaries are known. Several features are implemented to help verify the segmentation algorithm and to evaluate the feasibility of classifying different types of blood cells. These features include size, intensity, and shape measurements as well as ratios of these measurements.

Size features give an indication of how large each region of the cell is. These measurements include the area and perimeter of the cell, the cytoplasm, and the nucleus. The area measurement is obtained by determining the number of points in the specific region (cell, nucleus or cytoplasm) as defined by its image mask M(x,y), in a 64 pixel by 64 pixel matrix, i.e.

$$\text{Area} = \sum_{x=0}^{63} \sum_{y=0}^{63} M(x,y) \tag{19}$$

where M(x,y) is the cell mask and has a value of 1 in the object and 0 elsewhere.

The perimeter measurement is obtained using the information from the chain code. The chain code, described in Chapter 4.5, contains odd, even and corner elements of the edge. A weighted sum of the number of these elements is used to determine the perimeter. This method will give a more accurate perimeter value for circularly shaped objects since it compensates for edges which do not align with the square image grid. The formula developed by Young (1988) is used since it is optimized for the perimeter of circular objects, i.e.

$$\text{Perimeter} = 1.406\ N_{odd} + 0.980\ N_{even} - 0.091\ N_{corner} + 2\sqrt{2} \qquad (20)$$

The ratio of areas of the nucleus to the cytoplasm is used to give an indication of the proportion of the different regions in the cell.

Intensity features give an indication of the amount of stain that is associated with the nucleus of the cell. The measurements used are the sample mean intensity I_{mean}, and the sample variance of intensity I_{var} in each of the three colour spectrums (red, green, and blue), i.e.

$$I_{mean} = \sum_{x=0}^{63} \sum_{y=0}^{63} \frac{I(x,y)\ M(x,y)}{\text{Area}} \qquad (21)$$

$$I_{var} = \sum_{x=0}^{63} \sum_{y=0}^{63} \frac{[I(x,y) - I_{mean}]^2\ M(x,y)}{\text{Area}} \qquad (22)$$

Shape features give an indication of how the nucleus of the cell looks like. One such measurement is circularity, i.e.

$$\text{Circularity} = \frac{\text{Perimeter}^2}{4\pi \text{ Area}} \tag{23}$$

Chapter 5
Discussion and Results

5.1 Data Collection

In order to test the blood cell analysis algorithm, approximately 1000 cells from 10 slides of blood smears were used. These slides were obtained from the Children's Hospital of British Columbia in Vancouver and contained typical variations which can be expected in blood smear preparations. The classification of these slides was known since they had been prepared at least one year ago and the history and progress of each patient are known to-date.

To collect the cells, randomly chosen areas on the slide were brought to the microscope field of view, using the motorized x,y stage of the device. Each field was manually focussed to obtain the greatest contrast in the image as seen on the monitor. Spectral images were then acquired and the system was programmed to automatically find the nucleated cells and to perform the segmentation. The resulting boundaries were overlaid on the cell images and displayed on the monitor for visual inspection. The spectral images (each 64 pixels by 64 pixels), the nucleus and cytoplasm masks, and the location of the cell on the slide were stored for later observation. At the end of the search, each of the detected cells was manually classified by a pathologist into 19 groups (Appendix A). The cell classification was

used in conjunction with the values of the calculated features to determine if a correlation exists.

Slides 1, 3, 4, 5, 6, and 8 came from patients with acute lymphoblastic leukemia (ALL) and contain a large number of lymphoblast cells amongst the nucleated cell population. All these slides have lymphoblast cells of the classification of L1 type with the exception of slide 5 which has both the L1 and L2 sub-classification types. Slides 2 and 7 were from patients with acute myelogenous leukemia (AML) and they contain a large population of myeloblast cells. Slides 9 and 10 were from patients who had been treated for ALL and hence they contain a mixture of the 15 different classes of normal nucleated cells as well as some abnormal cells.

5.2 Detection Accuracies

An important aspect of blood cell analyzers is their ability to correctly detect all nucleated cells in a given field and eliminate all other debris. Any nucleated cells which are left undetected, especially those of a specific class, may generate results which indicate that the slide is normal where in fact it is not. Debris which are not eliminated from the analysis may produce results that indicate abnormality in the slide. Although this is not as serious an error as not detecting cells (false negatives), these slides will have to be manually examined to verify its normality.

All nucleated cells were correctly detected in the selected frames. Most debris have equal intensity in all colour spectra and hence were easily eliminated by the subtraction of the blue image from the red. Although there are many regions in the image which belong to parts of red blood cells, platelets, and other debris, these were generally very small and were eliminated by the erosion process and the size criteria imposed on each isolated object. Objects which are too large (such as clumps of cells) were also eliminated by the size criterion. Cells which were touching the borders of the image were not included in the data since there was not enough information to classify a fraction of a cell.

Of the 1078 detected nucleated cells, 781 were individual, single cells and 297 were two or three cells that were just touching each another. Of these touching cells, 271 were correctly divided into individual cells, 18 had minor errors in the position of the boundary, and 8 experienced major errors where the location of the boundary was misplaced (Figure 17).

Minor errors in separating touching cells is largely due to the boundary smoothing operation applied to the nucleated cell mask. This smoothing operation is performed to collect and merge any scattered pieces which belongs to the cytoplasm after the thresholding operation. As a result, the location where two cells touch is blurred. Hence, the touching cell separating algorithm can choose points which are upto 3 pixels away from the actual boundary position. This error can be corrected by

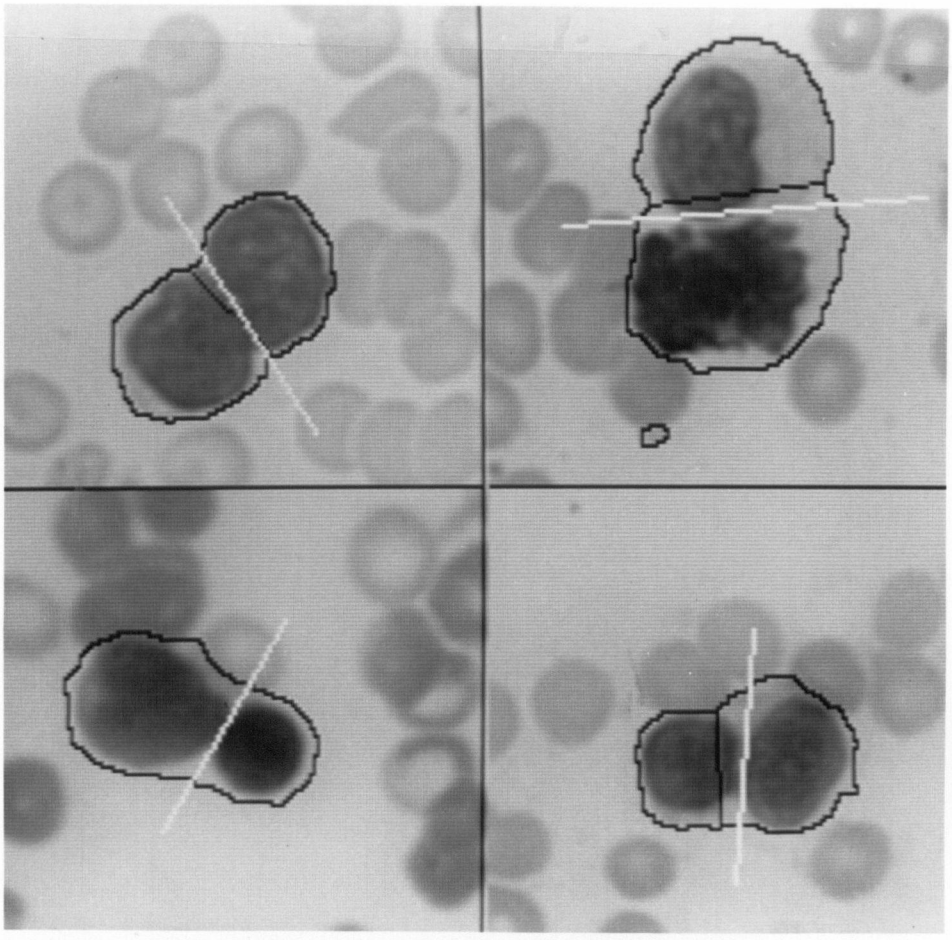

Figure 17

MINOR AND MAJOR ERRORS IN SEPARATING TOUCHING CELLS

The minor (top) and major (bottom) errors in separating touching cells is shown. The separating line produced by the algorithm is shown in black and the actual boundary location is shown in white. This line is slightly shifted in the case of the minor errors. Major errors *includes* those which are not separated or incorrectly separated.

introducing an algorithm which will search in the neighbourhood of the coarsely chosen cell separation point, using the intensities of the image and other criteria, to locate the exact dividing point.

Major errors are due to irregularly shaped (not elliptic) cells or cells which are near platelets or fragmented pieces of cytoplasm. The algorithm will either split the single cell into pieces or include fragments which do not belong to the cell into the nucleated cell mask. Some of these errors can be corrected for by analyzing the features of these objects.

5.3 Segmentation Accuracies

Another important criterion in analyzing blood cell images is the accuracy in defining the regions of the cell. The correctness of segmentation is crucial since the rest of the analysis is based on the defined regions. The results of the cells analyzed are tabulated in Tables I to V. Minor cytoplasm errors (Figure 18) are those errors where small fragments of the cytoplasm of the cell are not included in the region or too much of other areas, such as cytoplasm of another cell and background, are included in the defined cytoplasmic region. Minor nucleus errors (Figure 19) are those errors where parts of the cytoplasm are included or parts of the nucleus are not included in the nuclear region. The major reason for the large number of minor nucleus errors is the smoothing process which smooths out sharp concavities present in certain types of white blood cells.

Major cytoplasm errors (Figure 20) arise when cells are irregularly shaped or when the cytoplasm of some nucleated cells possess a colour very similar to that of the red blood cells and thus is eliminated from the cell mask. Major nucleus errors (Figure 21) are contributed to the uneven stain uptake in the cells. The cytoplasm of some cells incorporates too much stain resulting in a larger segmented nuclear region. Some nuclei have very dark stained regions and thus the algorithm assigns the lighter parts of the nucleus to the cytoplasm area.

The accuracy of the segmentation also depends on how well the cells are focussed. The focussing range is in the order of five microns at the chosen microscope setup. As the focus is changed, the transition of intensity levels at the nucleus and cytoplasm boundary is not abrupt enough and may result in errors in defining the nucleus region. The cytoplasm of the nucleated cells can also blend into the rest of the background causing cytoplasm segmentation errors.

As shown in the Tables I to V, the error rates in segmentation vary from slide to slide. This is due to the type of cells on the slide as well as the way the slide was prepared. In slides 9 and 10 which contain a mixture of the cell types in the blood, more cytoplasm related errors are present because there is a greater probability of finding cells which have a cytoplasm colour similar to the red blood cells compared to the other eight slides. The percentage of correct segmentation ranges

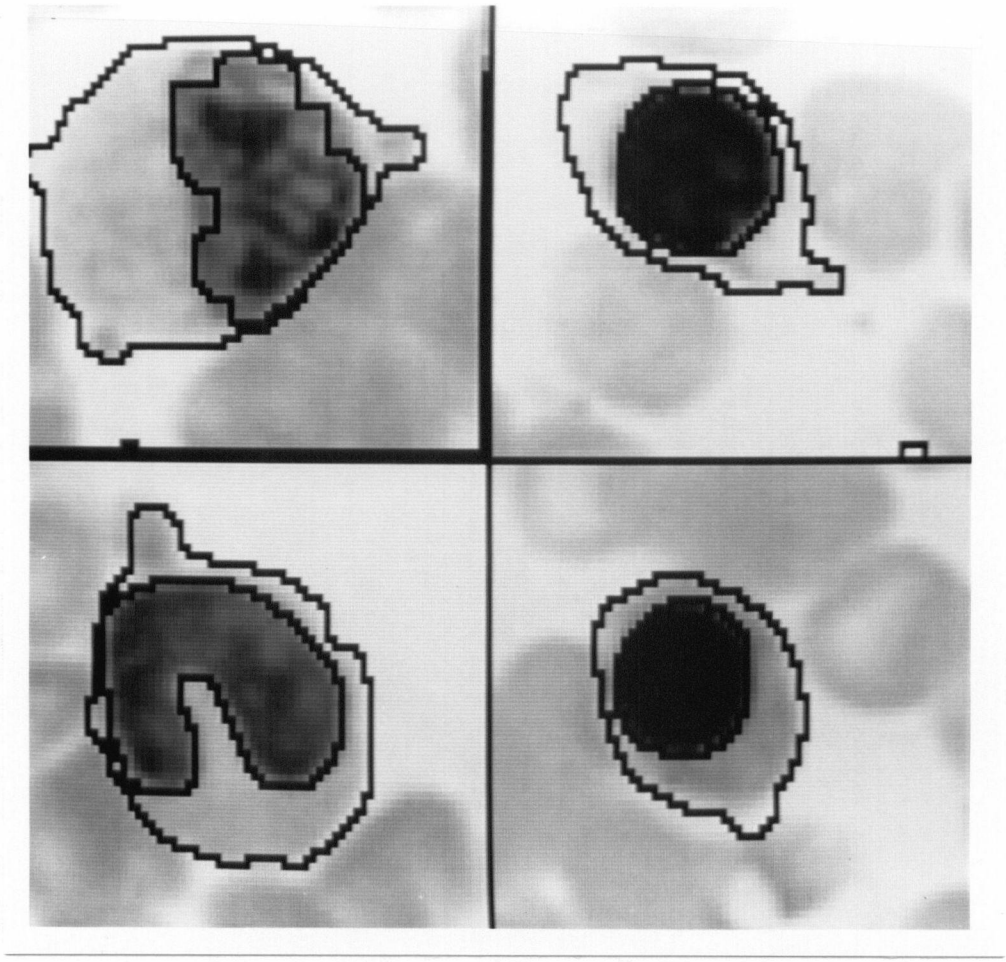

Figure 18

MINOR CYTOPLASM ERRORS

Examples of minor cytoplasm errors are shown. The algorithms either include small fragments of the background or other cells into the cytoplasm or exclude parts of its own cytoplasm.

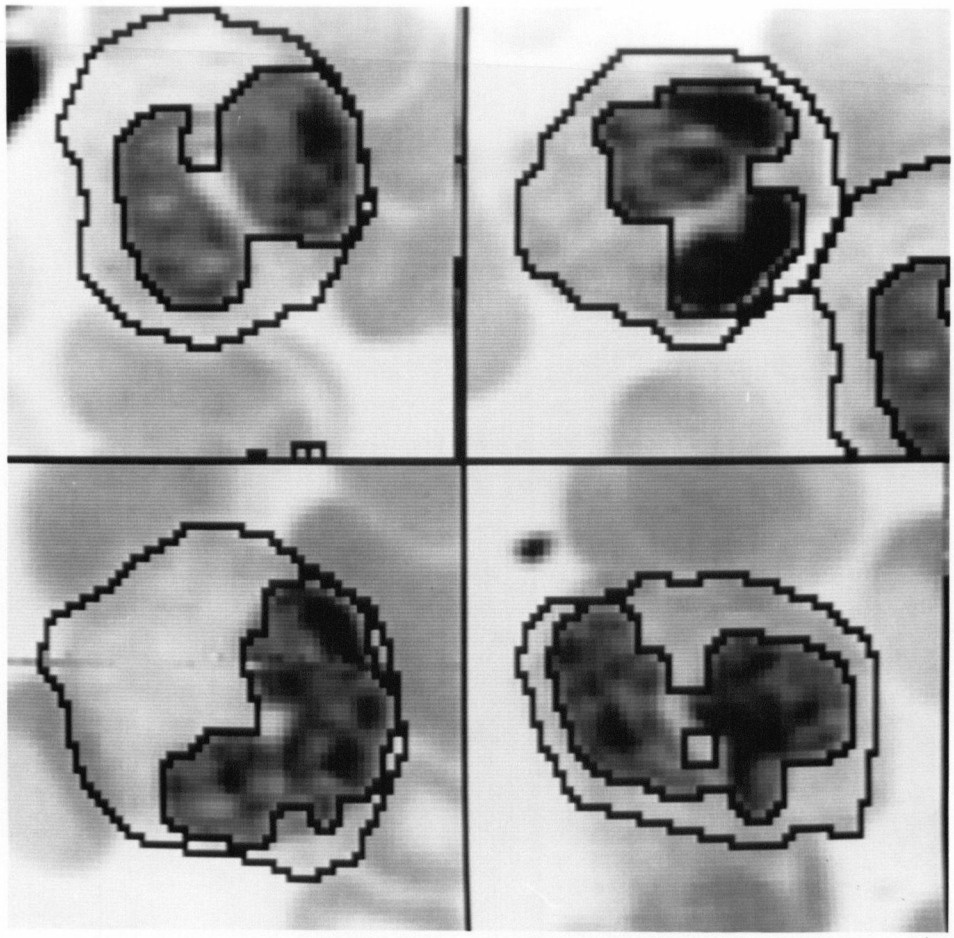

Figure 19

MINOR NUCLEUS ERRORS

Examples of minor nucleus errors are shown. The algorithms include parts of the cyotplasm into the nucleus region.

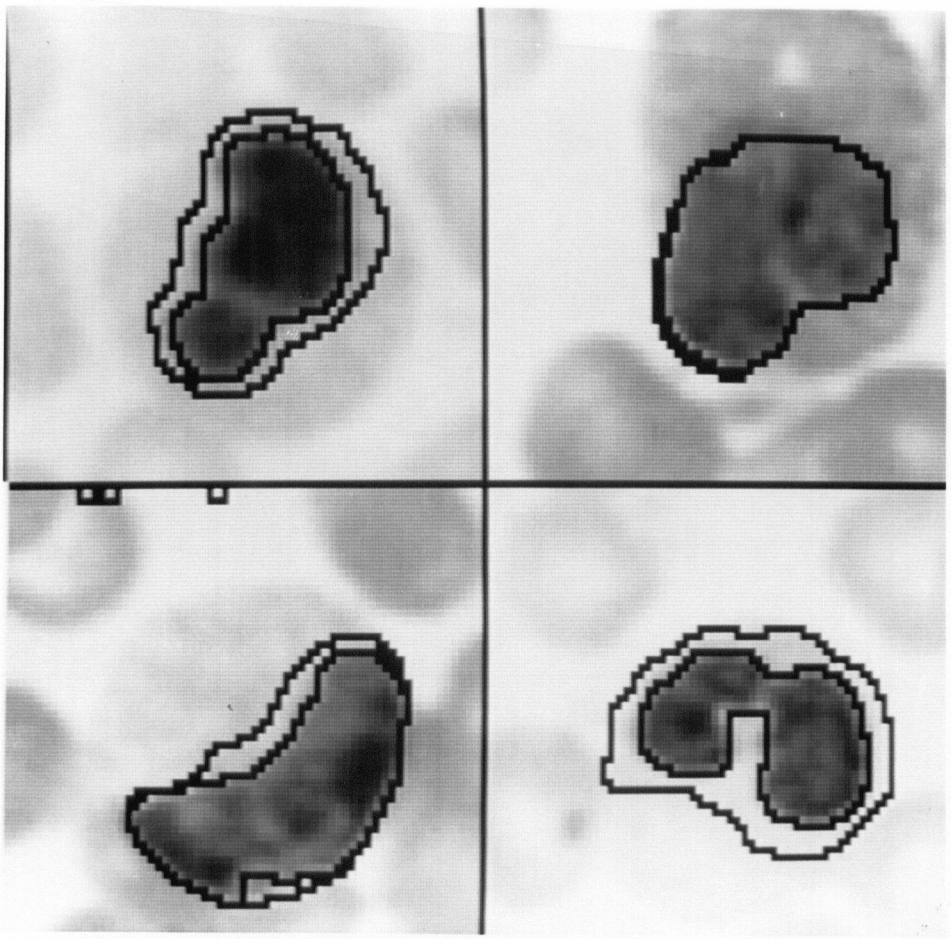

Figure 20

MAJOR CYTOPLASM ERRORS

Examples of major cytoplasm errors are shown. The algorithms exclude a major portion the cytoplasm of the cell from the cytoplasm region.

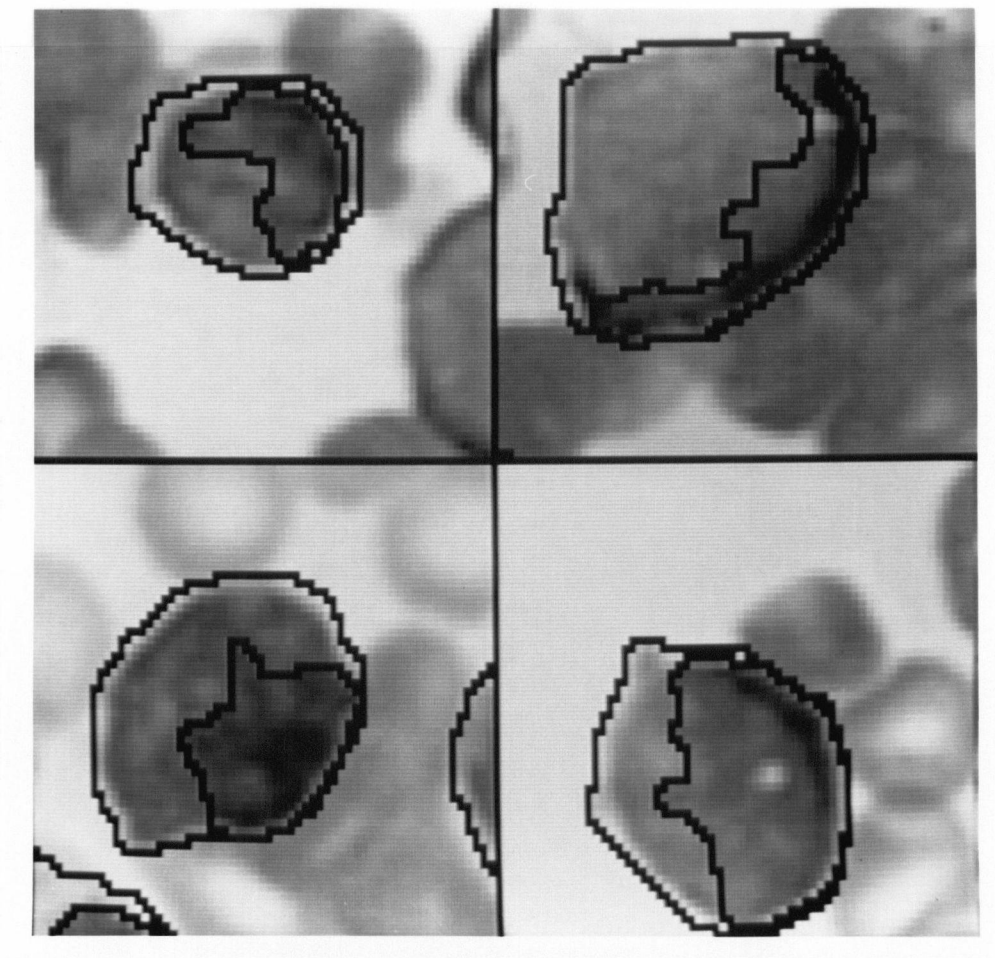

Figure 21

MAJOR NUCLEUS ERRORS

Examples of major nucleus errors are shown. The algorithms exclude a major portion of the nucleus.

Table I

SEGMENTATION ERRORS IN NON-TOUCHING NUCLEATED CELLS.

Slide Number	Correct Seg.	Minor Nucleus	Minor Cyto.	Major Nucleus	Major Cyto.	Major N & C	Total
1	82	7	2	5	2	2	100
2	93	10	0	0	0	0	103
3	63	2	2	0	2	0	69
4	72	6	0	0	0	0	78
5	68	2	3	11	0	0	84
6	67	2	1	0	0	0	70
7	58	7	1	8	0	0	74
8	59	2	3	2	0	0	66
9	56	1	1	2	5	1	66
10	58	0	4	2	7	0	71
Total	676	39	17	30	16	3	781

Table II

PERCENTAGE ERRORS IN NON-TOUCHING NUCLEATED CELLS.

(Table I represented as percentages)

Slide Number	Correct Seg.	Minor Nucleus	Minor Cyto.	Correct & Minor	Major Nucleus	Major Cyto.	Major N & C
1	82.0	7.0	2.0	91.0	5.0	2.0	2.0
2	90.3	9.7	0	100.0	0	0	0
3	91.3	2.9	2.9	97.1	0	2.9	0
4	92.3	7.7	0	100.0	0	0	0
5	81.0	2.4	3.6	87.0	13.1	0	0
6	95.7	2.8	1.4	100.0	0	0	0
7	78.4	9.4	1.4	89.2	10.8	0	0
8	89.4	3.0	4.6	97.0	3.0	0	0
9	84.8	1.5	1.5	87.8	3.0	7.6	1.5
10	81.7	0	5.6	87.3	2.8	10.0	0
Total	86.4	5.0	2.2	93.6	3.8	2.0	0.4

Table III

SEGMENTATION ERRORS IN TOUCHING NUCLEATED CELLS.

Slide Number	Correct Seg.	Minor Nucleus	Minor Cyto.	Major Nucleus	Major Cyto.	Major N & C	Total
1	8	0	1	1	0	0	10
2	3	0	0	0	0	0	3
3	35	0	0	1	3	0	39
4	23	0	2	1	0	0	26
5	24	1	0	3	0	0	28
6	29	2	2	0	0	0	33
7	30	5	0	0	0	0	35
8	35	8	3	1	0	0	47
9	31	0	5	1	2	0	39
10	29	0	5	0	3	0	37
Total	247	16	18	8	8	0	297

Table IV

PERCENTAGE ERRORS IN TOUCHING NUCLEATED CELLS.

(Table III represented as percentages)

Slide Number	Correct Seg.	Minor Nucleus	Minor Cyto.	Correct & Minor	Major Nucleus	Major Cyto.	Major N & C
1	80.0	0	10.0	90.0	10.0	0	0
2	100.0	0	0	100.0	0	0	0
3	89.7	0	0	89.7	2.6	7.7	0
4	88.5	0	7.7	96.2	3.8	0	0
5	85.7	3.6	0	89.3	10.7	0	0
6	87.9	6.1	6.1	100.0	0	0	0
7	85.7	14.3	0	100..0	0	0	0
8	74.5	17.0	6.4	87.9	2.1	0	0
9	79.5	0	12.8	92.3	2.6	5.1	0
10	78.4	0	13.5	91.9	0	8.1	0
Total	83.2	5.4	6.1	94.6	2.7	2.7	0

Table V

PERCENTAGE SEGMENTATION ERRORS IN NUCLEATED CELLS.

(Tables I and III combined and represented as percentages)

Slide Number	Correct Seg.	Minor Nucleus	Minor Cyto.	Correct & Minor	Major Nucleus	Major Cyto.	Major N & C
1	81.8	6.4	2.7	90.9	5.5	1.8	1.8
2	90.6	9.4	0	100.0	0	0	0
3	90.7	1.9	1.9	94.5	0.9	4.6	0
4	91.3	5.8	1.9	99.0	1.0	0	0
5	82.1	2.7	2.7	87.5	12.5	0	0
6	93.2	3.9	2.9	100.0	0	0	0
7	80.7	11.0	1.0	92.7	7.3	0	0
8	83.2	8.8	5.3	97.3	2.7	0	0
9	82.9	0.9	5.7	89.5	2.9	6.4	0.9
10	80.6	0	8.3	88.9	1.9	9.2	0
Total	85.4	5.1	3.2	94.0	3.5	2.2	0.3

from 80.6% to 93.2%. The range of percentages for minor errors in the nucleus is 0% to 11.0%, minor error in the cytoplasm is 0% to 8.3%, major errors in the nucleus is 0% to 12.5%, and major errors in the cytoplasm is 0% to 1.8%.

5.4 Feature Calculation Accuracies

Features are calculated from the regions defined by the segmentation process. Even if there were no errors in the segmentation, there will be errors introduced in tessellating the image to a square-pixel grid, and errors introduced in the method used to calculate a feature. To illustrate these errors, a test image consisting of a circle is tessellated at different resolutions and the area feature is calculated. The circle image is generated by assigning all points in the grid which satisfies the equation to a value of 1 and all other pixels to a value of zero, i.e.

$$(x - x_c)^2 + (y - y_c)^2 < \text{square radius of circle} \qquad (24)$$

where x_c and y_c are the coordinates of the centre of the circle and x and y are the location in the grid.

The area feature is calculated by counting the number of 1's in the image. Since the position of a cell can lie anywhere in the image, the position of the circle is allowed to randomly vary within a pixel spacing. A plot of the percentage error from the actual value is shown

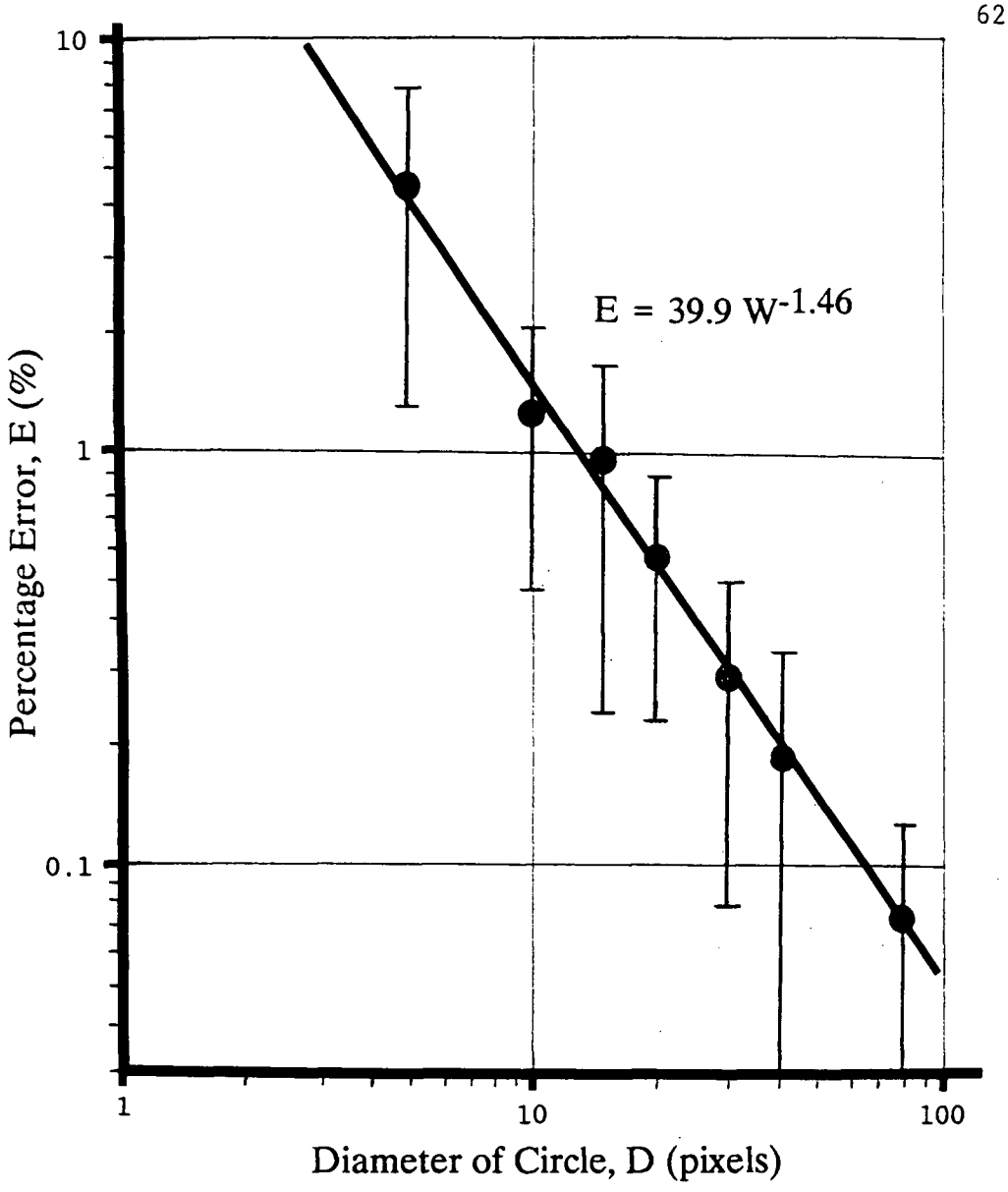

Figure 22

FEATURE CALCULATION ACCURACIES

The percentage errors in calculating the area of a circle using different number of pixels to represent the circle is shown. It can be seen that the error decreases as more pixels are used to represent the circle.

in Figure 22. It can be seen that if the diameter of the circle spans more than ten pixels in width, an error of less than two percent in the area calculation can be obtained.

Although there are errors in the calculation of features, as long as their distribution for a certain class of cell does not conflict with other classes, the error will not be significant in classifying the cell type.

5.5 Cell Classification

The nucleated cells, which were detected and segmented, were classified by an experienced pathologist into approximately 20 groups. Simple features were calculated from these cells and are used to determine the classification of certain types of cells. Some cell types which are identified based on their colour information, such as the polychromatophilic normoblast and basophilic normoblast, can be separated using the mean intensities of the cytoplasm in the red and green spectrums (Figure 23). Other types of cells, such as the lymphoblast and myeloblast, can be separated using the perimeter of the nucleus and the ratio of the nucleus to cell area features (Figure 24). It is evident from plots of the calculated features (Figures 23 and 24) that clusters of certain classes are present. This verifies that the methods used to segment the regions and the calculations of the feature values for these classes are sufficient in determining the correct classification of some types of nucleated cell. Although more features

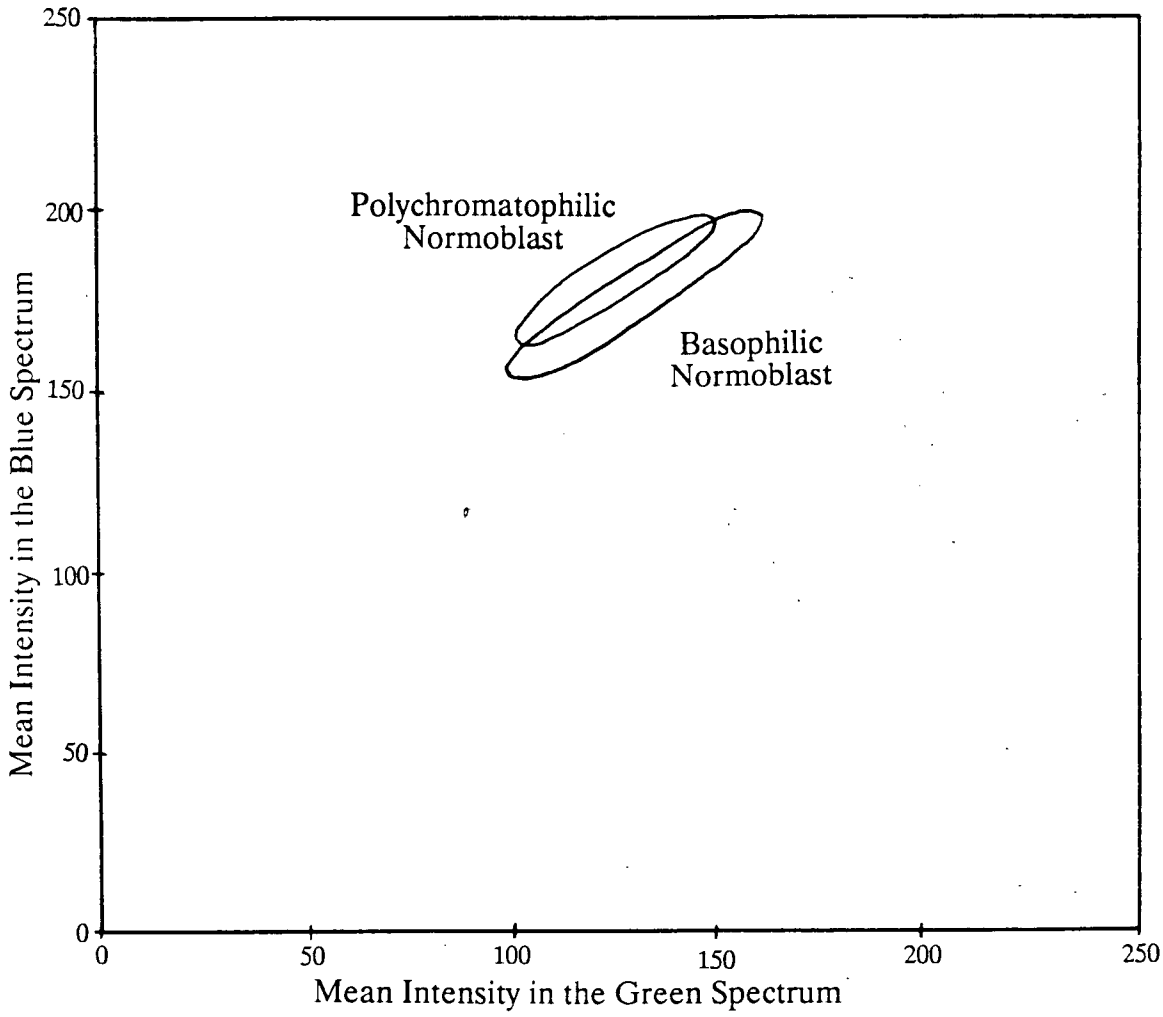

Figure 23

CLUSTER PLOT OF THE MEAN INTENSITIES

A cluster plot displaying the mean intensities in the green and blue spectrums of the images of two classes of blood cells: polychromatophilic normoblast and basophilic normoblast.

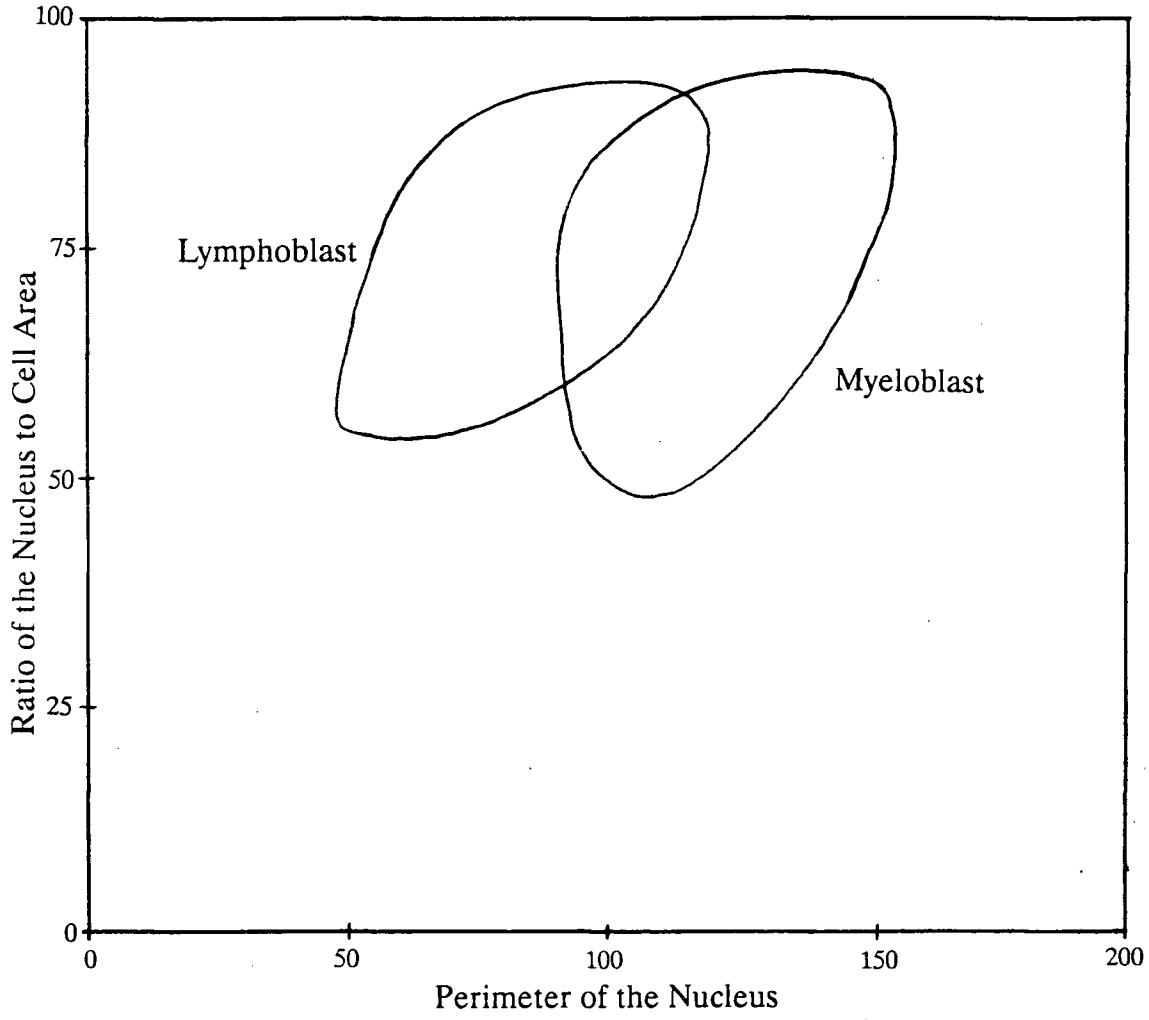

Figure 24

CLUSTER PLOT OF THE PERIMETER AND RATIO OF AREAS

A cluster plot displaying the perimeter of the nucleus and the ratio of the nucleus to cell area of images of two classes of malignant blood cells: lymphoblast and myeloblast.

and multi-dimensional cluster analysis algorithms are required to separate the different classes of cells, it is unnecessary to add additional algorithms to fine tune the boundaries of the segmented regions.

Chapter 6
Conclusion and Future Suggestions

6.1 Overview

The algorithms to i) capture and calibrate the image, ii) detect and segment the cells in the image, iii) generate features from the segmented regions, and iv) classify the cells based on the feature values, have been shown to be useful in the analysis of nucleated blood cells. Techniques of image averaging and background subtraction are first employed to improve the quality of the input image. The new method of subtracting spectral images is shown to be very useful in generating bi-modal grey level histogram of the resulting image where smoothing and threshold detection techniques are subsequentially employed to separate the nucleated cells from the rest of the image. The new method of using the difference in angles along the boundary of the binary image to separate touching cells has allowed more cells to be analyzed from the chosen areas of the slide. The conditional mean filter has produced images where the nucleus and cytoplasm boundary is more readily defined. Finally, erosion and dilation operations were found to adequately fill the holes in the regions and smooth the region boundaries. Once, the regions are defined, various features can be calculated. These feature values are then compared to determine if there are any groupings amongst the different classes of cells.

It is evident from the survey of cytometry systems that blood cell analysis is important in medical practice and that all of these systems have difficulty in classifying abnormal blood cells. Hence, the Cell Analyzer Imaging System was used as the tool to develop and test the algorithms discussed in this thesis. The survey of segmentation algorithms employed to segment blood cells confirmed that no particular single algorithm will work on all images. However, combining several different algorithms may perform well; the algorithms which work are those which are tailored to a particular type of images one obtains.

6.2 System Performance

The algorithms perform well in analyzing the types of cells in a blood smear. Of the 1078 cells chosen, 3% of the 297 touching cells were not properly separated due to the odd cell shape. Although the boundary for 6% of these touching cells is slightly misplaced, these cells were still properly classified based on their feature values. 6% of the 781 single cells were incorrectly segmented and 7% have slight errors. Although there are minor errors in the segmentation, the distribution of features extracted indicates that different classes of blood cells can be distinguished.

6.3 Future Plans

The algorithms developed in this thesis permit classification of several types of different white blood cells. To discriminate between more

classes and subclasses of blood cells, more features, based on the segmented areas, would have to be developed and incorporated in the algorithm. Features such as the mean and variance of intensity levels at different wavelengths and their ratios may be used. Texture features which give an indication of how intensity levels are varying in a region are also good features to incorporate.

Once a collection of more than 20 features are calculated for each cell, a criterion must be developed to interpret the feature values and use it to classify the cells on the slide (Poon, Jaggi and Palcic, 1987). A linear stepwise discriminant function analysis should be perform on the feature values to select the features which would best separate the different classes of cells. Experimentation in the removal of those features, which are computationally expensive, from the analysis should be investigated to determine its effects on the classification errors. Algorithms should also be developed to detect and discard cells that are not segmented properly based on these feature values.

Since the sharpness and contrast of the images are dependent on the focus, an important feature that must be developed is autofocus (Poon et al., 1989). An autofocussing system will produce an objective and consistent level of focus from one image to the next based on some pre-determined criteria, whereas a subjective level of focus (which might vary from image to image) would be chosen if human intervention is involved. A criterion, such as the sum of the absolute intensity gradients in the image can be used to give an indication of the focus

level. A high value for the sum will indicate that there is large variations in intensity (details) in the image which is characteristic of a focussed image. Thus, the system will determine the optimum focus level based on the feature values obtained at different focus levels, and instruct the stepping motors to adjust the focus before the cell detection and segmentation algorithms are initiated.

Using these additional algorithms, a fully automated blood cell analyzing system can be developed to classify the blood cells on the slide. The system should include a motorized x,y stage to scan the slide and a mechanism and algorithm to automatically focus the cells on the slide. An automatic slide loader should also be incorporated to place the slide on the motorized stage and to place those slides which are suspected of being abnormal in a different place for future manual observation and verification of the machine classification. This system would allow hospitals to scan a large number of slides quickly with little human interaction, as well as generating a standard in classifying abnormal slides.

6.4 Summary of Author's Contributions

The Cell Analyzer Imaging System has been built to analyze stained cells, under the supervision of Branko Palcic and Bruno Jaggi. The author of this thesis has played a major role in the development of this system, including hardware, device drivers, and software (Jaggi, Poon and Palcic, 1986; Poon, Jaggi and Palcic, 1987; Palcic et al., 1988;

Jaggi et al., 1988; Poon et al., 1989; Poulin et al., 1989; Spadinger, Poon and Palcic, 1989a; and Spadinger, Poon and Palcic, 1989b). The development of the system was designed to allow work to be performed as presented in this thesis.

Using this system, a procedure containing algorithms for automatic segmentation of nucleated blood cells was developed by the author. This included the methods of image acquisition, corrections, and subtraction, and binary mask processing which were modified and adapted into the cell analysis procedure. New methods, using the difference angles to separate touching cells and the conditional mean filter to reduce intensity variations while preserving edges, were introduced and also incorporated into the procedure. A test data set of over 1000 cells was used to evaluate the segmentation algorithms.

The main contribution to new knowledge in this field, apart from introducing several new algorithms, is to combine the hardware and algorithms into a working system which allows scientists in the medical field related to leukemia diseases to study this disease in much greater detail than was possible before.

Chapter 7

Bibliography

Abmayr W., Mannweiler E., Oesterle D., and Deml E. (1987) Segmentation of scenes in tissue sections. Analytical and Quantitative Cytology and Histology, 9:190-196

Amadasun M., and King R.A. (1988) Low-level segmentation of multispectral images via agglomerative clustering of uniform neighbourhoods. Pattern Recognition, 21(4):261-268.

Arcelli C., Cordella L.P., and Levialdi S. (1981) From local maxima to connected skeletons. Pattern Analysis and Machine Intelligence, 3(2):134-143

Arcelli C., and Di Baji G.S. (1978) On the sequential approach to medial line transformation. Systems, Man, and Cybernetics, 8(2):139-144

Aus H.M., Harms H., Haucke M., Beritova J., Ter Meulen V., Gunzer U., Baumann I., and Abmayr W. (1986) Leukemia-related morphological features in blast cells. Cytometry, 7:365-370

Aus H.M., Ruter A., Ter Meulen V., Gunzer U., and Nurnberger R. (1977) Bone marrow cell scene segmentation by computer-aided color cytophotometry. The Journal of Histochemistry and Cytochemistry, 25(7):662-667

Bacus J.W. and Grace L.J. (1987) Optical microscope system for standardized cell measurements and analyses. Applied Optics, 26(16):3280-3293

Bacus J.W., Gose E.E. (1972) Leukocyte Pattern Reognition. Systems, Man, and Cybernetics, 2(4):513-536

Begemann H., and Rastetter J. (1979) Atlas of Clinical Hematology. Third Edition, Springer-Verlay, Berlin.

Bengtsson E., Eriksson O., Holmquist J., Jarkrans T., Nordin B., and Stenkvist B. (1981) Segmentation of cervical cells: detection of overlapping cell nuclei. Computer Graphics and Image Processing, 16:382-394

Bengtsson E., Eriksson O., Holmquist J., Nordin B., and Stenkvist B. (1979) High resolution segmentation of cervical cells. The Journal of Histochemistry and Cytochemistry, 27(1):621-628

Bengtsson E., Eriksson O., Holmquist J., and Stenkvist B. (1979) Implementation and Evaluation of a Diode Array Scanner for Digitizing Microscopic Images. The Automation of Cancer Cytology

and Cell Image Analysis. Eds. Pressmann N.J. and Wied S.L., 269-289

Bennett J.M., Catovsky D., Daniel M.T., Flandrin G., Galton D.A.G., Gralnick H.R., and Sultan C. (1976) Proposal for the Classification of the Acute Leukemias: French-American-British (FAB) cooperative group. British Journal of Hematology, 33:451-458

Brenner J.F., Necheles T.F., Bonacossa I.A., Fristensky R., Weintraub B.A., and Neurath P.W. (1977) Scene segmentation techniques for the analysis of routine bone marrow smears from acute lymphoblastic leukemia patients. The Journal of Histochemistry and Cytochemistry, 25(7):601-613

Castleman K.R. (1987) Spatial and photometric resolution and calibration requirements for cell image analysis instruments. Applied Optics, 26(10):3338-3342

Castleman K.R. (1979) Digital Image Processing. Prentice Hall, New York

Cheng G.C. (1974) Color information in blood cells. The Journal of Histochemistry and Cytochemistry, 22(7):517-521

Clark M, Bovik A.C., and Geisler W.S. (1987) Texture segmentaion using Gabor modulation /demodulation. Pattern Recognition Letters, 6:261-267

Davis L.S. (1975) A survey of edge detection techniques. Computer Graphics and Image Processing, 4:248-270

Dill A.R., Levine M.D., and Noble P.B. (1987) Multiple resolution skeletons. Pattern Analysis and Machine Intelligence, 9(4):495-503

Dytch H.E., Bibbo M., Bartels P.H., Puls J.H., and Wied G.L. (1987) A PC-based system for the objective analysis of histologic specimens through quantitative contextual karyometry. Applied Optics, 26(16):3270-3279

Fu K.S., and Mui J.K. (1981) A survey of image segmentation. Pattern Recognition, 13:3-16

Fulwyler M.F. (1965) Electronic Separation of Biological Cells by Volume, Science, 150:910

Garbay C., Chassery J.M., and Brugal G. (1986) An iterative region-growing process for cell image segmentation based on local color similarity and global shape criteria. Analytical and Quantitative Cytology and Histology, 8:25-34

Graham M.D., and Norgren P.E. (1980) The Diff3 Analyzer: A Parallel/Serial Golay Image Processor, Real-Time Medical Image Processing. Onoe M., Preston K. Jr., and Rosenfeld A. Eds. Plenum, New York.

Hadon J.F. (1988) Generalised threshold selection for edge detection. Pattern Recognition, 21(3):195-203

Hall T.L., Keyani D.H.L., and Rosenthal D.L. (1987) Microcomputer-based image processing workstations for cytology. Applied Optics, 26(16):3266-3269

Haralick R.M., Sternberg S.R., and Zhuang X. (1987) Image analysis using mathematical morphology. Pattern Analysis and Machine Intelligence, 9(4):532-550

Harms H., Aus H.M., Haucke M., and Gunzer U. (1986) Segmentation of stained blood cell images measured at high scanning density with high magnification and high numerical aperture optics. Cytometry, 7:522-531

Haussmann G. and Liedtke C.E. (1984) A region extraction approach to blood smear segmentation. Computer Vision, Graphics, and Image Processing, 25:133-150

Ingram M., and Preston K.Jr. (1970) Automatic Analysis of Blood Cells. Scientific America, 223:72-82

Inoue S. (1986) Video Microscopy. Plenum, New York, 1986.

Jaggi B., Poon S.S.S., MacAulay C., and Palcic B. (1988) Imaging System for Morphometric Assessment of Conventionally and Fluorescently Stained Cells. Cytometry, 9:6

Jaggi B., and Palcic B. (1985) The Design and Development of an Optical Scanner for Cell Biology. IEEE Proceedings, Engineering in Medicine and Biology, 2:980-985

Jaggi B., Poon S.S.S., and Palcic B. (1986) Implementation and Evaluation of the Dmips Cell Analyzer. IEEE Proceedings, Engineering in Medicine and Biology, 3:906-911

Kasdan H.L., Lanford K.C., Liberty J., Zachariash M., and Diendoerfer F.H. (1987) High performance pathology workstation using an automated multispectral microscope. Applied Optics, 26(16):3294-3300

Lacroix V. (1988) A three-model strategy for edge detection. Pattern Analysis and Machine Intelligence, 10(6):803-810

Landeweerd G.H., Timmers T., and Gelsema E.S. (1983) Classification of normal and abnormal samples of peripheral blood by linear mapping of the feature space. Pattern Recognition, 16(3):319-326

Landeweerd G.H., Gelsema E.S., Brenner J.F., Selles W.D., and Zahniser D.J. (1983) Pattern recognition of nucleated cells from the peripheral blood. Pattern Recognition, 16(2):131-140

Lee J.S. (1983) Digital Image Smoothing and the Sigma Filter. Computer Vision, Graphics, and Image Processing, 24:255-269

Lemkin P., and Lipkin L. (1979) Use of the positive difference transform for RBC elimination in bone marrow smear images. Analytical and Quantitative Cytology, 1:67-76

Lesty C., Raphael M., Nonnenmacher L., Leblond-Missenard V., Delcourt A., Homond A., and Binet J.L. (1986) An application of mathematical morphology to analysis of the size and shape of nuclei in tissue sections of non-Hodgkin's lymphoma. Cytometry, 7:117-131

Liedtke C.E., Gahn T., Kappei F., and Aeikens B. (1987) Segmentation of Microscopic cell scenes. Analytical and Quantitative Cytology and Histology, 9:197-211

Lin Y.K., and Fu K.S. (1981) Segmentation of Papanicolaou smear images. Analytical and Quantitative Cytology, 3:201-206

MacAulay C., and Palcic B. (1988) A comparison of some quick and simple threshold selection methods for stained cells. Analytical and Quantitative Cytology, 10:134-138

Mantas J. (1987) Methodologies in pattern recognition and image analysis - a brief survey. Pattern Recognition, 20(1):1-6

Marr, D. (1982) Vision, W.H. Freeman and Company, New York

Mastin G.A. (1985) Adaptive filters for digital image noise smoothing: an evaluation. Computer Vision, Graphics, and Image Processing, 31:103-121

Miller D.R., Leikin S., Albo V., Sather H., Karon M., Hammond D. (1981) Prognostic Importance of Morphology (FAB Classification) in Childhood Acute Lymphoblastic Leukemia (ALL). British Journal of Hematology, 48:199-206

Megla G.K. (1973) The LARC automatic white blood cell analyzer: Acta Cytologica, 17(1):3-14

Mui J.K., Fu K.S., and Bacus J.W. (1977) Automated classification of blood cell neutrophils. The Journal of Histochemistry and Cytochemistry, 25(7):633-640

Norgren P.E., Kulkarni A.V., and Graham M.D. (1981) Leukocyte image analysis in the diff3 system. Pattern Recognition, 13(4):299-314

Ohlander R., Price K., and Reddy R. (1978) Picture segmentation using a recursive region splitting method. Computer Graphics and Image Processing, 8:313-333

Pal S.K., and Pal N.R. (1987) Segmentation based on measures of contrast, homogeneity, and region size. IEEE Transanctions on Systems, Man, and Cybernetics, 17(5):857-868

Palcic B. and Jaggi B. (1989) Image Cytometry System for Morphometric Measurements of Live Cells. Bio-instrumentation: Developments and Applications. Ed. Wise D.L., Butterworth Publishers, Stoneham, MA.

Palcic B., Poon S.S.S., Thurston G. and Jaggi B. (1988) Time lapse records of cells in vitro using optical memory disk and Cell Analyzer. Journal of Tissue Culture Methods, 11(1):19-22.

Palcic B., Jaggi B. and Nordin J.A. (1987) Dynamic Microscope Image Processing Scanner. United States Patent #4,700,298.

Philip J. and Lundsteen C. (1985) Semiautomated Chromosome Analysis: A Clinical Test, Clinical Genetics, 27:140-146

Poon S.S.S., Jaggi B., and Palcic B. (1987) Cell Recognition Algorithm for the Cell Analyzer. IEEE Proceedings, Engineering in Medicine and Biology, 3:1455-1456

Poon S.S.S., Jaggi B., Spadinger I., and Palcic B. (1989) Focussing methods used in the Cell Analyzer. IEEE Proceedings, Engineering in Medicine and Biology, (in press)

Poulin N., Poon S.S.S., Kandola G. and Palcic B. (1989) Automatic detection of metaphase chromosomes. IEEE Proceedings, Engineering in Medicine and Biology (in press).

Pratt W.K. (1978) Digital Image Processing. John Wiley & Sons, New York

Preston K.Jr. (1987) High-resolution leukocyte analyzers: retrospective and prospective. Applied Optics 26(16):3258-3265

Preston K.Jr. (1980) Automation of the analysis of cell images. Analytical and Quantitative Cytology, 2:1-14

Preston K.Jr. (1976) Digital Picture Analysis in Cytology, Digital Picture Analysis. Ed. Rosenfeld A., Springer Verlay, New York, 209-293

Rosenfeld A., and Kak A.C. (1982) Digital Picture Processing. Second Edition, Volume 2. Academic Press, New York

Schwartz M., and Shaw L. (1975) Signal Processing: Discrete Spectral Analysis, Detection, and Estimation. McGraw-Hill, New york

Shoemaker R.L., Bartels P.H., Hillman D.W., Jones J., Kessler D., Shack R.V., and Vukobratovich D. (1982) An Ultrafast Laser Scanner Microscope for Digital Image Analysis, IEEE Transactions on Biomedical Engineering, BME29(2):82-91

Spadinger I., Poon S.S.S. and Palcic B. (1989a) Automated detection and recognition of live cells in tissue culture using image cytometry. Cytometry (in press).

Spadinger I., Poon S.S.S. and Palcic B. (1989b) Effect of focus on cell detection and recognition by the Cell Analyzer. Cytometry (submitted).

Tanaka N., Ikeda H., Ueno T., Mukawa A., Watanabe S., Okamoto K. Hosoi S., and Tsunekawa S. (1987) Automated cytologic screening system (CYBEST model 4): an integrated image cytometry system. Applied Optics, 26(16):3301-3307

Tucker J.H., Husain O.A.N., Watts K., Farrow S., Bayley R., and Stark M.H. (1987) Automated densitometry of cell populations in a continuous-motion imaging cell scanner. Applied Optics, 26(10):3315-3324

Tucker J.H. (1979) An Image Analysis System for Cervical Cytology Automation Using Nuclear DNA Content, The Journal of Histochemistry and Cytochemistry 27(1):613-620

Tyrer H.W., and Pressman N.J. (1987) Strategies for automated placement of cells for microscopy. Applied Optics, 26(10):3308-3314

Umesh R.M. (1988) A technique for cluster formation. Pattern Recognition, 21(4):393-400

Walton W.H. (1952) Automatic Counting of Microscope Particles, Nature, 169

Wermser D., Haussmann G., and Liedke C.E. (1984) Segmentation of blood smears by Hierarchial thresholding. Computer Vision, Graphics, and Image Processing, 25:151-168

Young I.T. (1972) The classification of white blood cells. IEEE Transactions on Biomedical Engineering, 19(4):291-298

Young I.T., and Paskowitz I.L. (1975) Localiztion of cellular structures. IEEE Transactions on Biomedical Engineering, 22(1): 35-40

Young I.T. (1988) Sampling Density and Quantitative Microscopy, Analytical and Quantitative Cytology and Histology, 4:269-275

Young J.Z. and Roberts F. (1951) A Flying Spot Microscope, Nature, 167:231

Young T.Y., and Fu K.S., Eds. (1986) Handbook of Pattern Recognition and Image Processing. Academic Press, London

Zahniser D.J., Brenner J.F., and Selles W.D. (1986) Spectral bandwidth in automated leukocyte classification. Cytometry, 7:518-521

Zucker-Franklin D., Greaves M.F., Grossi C.E., and MArmont A.M. (1988) Atlas of Blood Cells: Function and Pathology. Second Edition, Edi. Ermes, Milan.

Appendix A

The nucleated blood cells are classified into the groups with the following codes. Objects with codes '0' to '9' and 'a' to 'c' belong to the normal blood cells and objects with codes 'f', 'g', and 'h' belong to the malignant blood cells.

Code	Cell Classification
-	dead cell
+	ignore (too difficult to classify)
0	neutophil
1	band
2	metamyelocyte
3	myelocyte
4	promyelocyte
5	blast
6	orthochronic normoblast
7	polychromatophilic normoblast
8	basophilic normoblast
9	pronormoblast
a	lymphocyte
b	monocyte
c	plasma cell
d	megakaryocyte
e	macrophage
f	lymphoblast L1
g	lymphoblast L2
h	myeloblast

Refer to Zucker-Franklin et al. (1988) and Begemann and Rastetter (1979) for examples and a description of these different cell types.

PUBLICATIONS:

1. Jaggi, B., Poon, S. and Palcic, B.: Implementation and evaluation of the DMIPS Cell Analyser. IEEE Proceedings, Engineering in Medicine and Biology 3: 906-911, 1986.

2. Jaggi, B., Poon, S. and Palcic, B.: Optical Memory Disks in Image Database Management for Cytometry. Applied Optics publ. by Optical Society of America 26: 3325-3329, 1987.

3. Poon, S.S.S., Jaggi, B. and Palcic, B.: Cell recognition algorithms for the Cell Analyser. IEEE Proc. Eng. Biol. 3: 1454-1456, 1987.

4. Palcic, B., Poon, S.S.S., Thurston, G. and Jaggi, B.: Time lapse records of cells in vitro using optical memory disk and Cell Analyzer. J. Tissue Culture Methods 11(1):19-22, 1988.

5. Jaggi, B., Poon, S.S.S., MacAulay, C. and Palcic, B.: Imaging system for morphometric assessment of conventionally and fluorescently stained cells. Cytometry 9:566-572, 1988.

6. Spadinger, I., Poon, S.S.S. and Palcic, B.: Automated detection and recognition of live cells in tissue culture using image cytometry. Cytometry. (In press, 1989).

7. Poon, S.S.S., Jaggi, B., Spadinger, I. and Palcic, B.: Focussing methods used in the cell analyzer. Proc. 11th IEEE Eng. Med. Biol. Soc., Seattle, WA., Nov. 8-12, 1989 (Accepted).

SUBMITTED PAPERS:

1. Poon, S.S.S., Jaggi, B., Spadinger, I., Palcic, B.: Focussing methods used in the Cell Analyzer. IEEE Proc. Eng. Med. Biol., 1989 (submitted).

2. Poulin, N., Poon, S.S.S., Kandola, G., Palcic, B.: Automatic detection of metaphase chromosomes. IEEE Proc. Eng. Med. Biol., 1989 (submitted).

3. Spadinger, I., Poon, S.S.S. and Palcic, B.: Effect of focus on cell detection and recognition by the cell analyzer. Cytometry 1989 (submitted).

REPORTS AND ABSTRACTS:

1. Jaggi, B., Poon, S. and Palcic, B.: Implementation and evaluation of the DMIPS Cell Analyser. IEEE Soc. Conference, Dallas-Fort Worth, Texas, November 7-10, 1986.

2. Palcic, B., Poon, S.S.S. and Jaggi, B.: The development of the Cell Analyzer for use in analytical cytology. 1st Int'l. Conference on Artificial Intelligence Systems, Los Angeles, February 1-3, 1987.

3. Poon, S.S.S., Jaggi, B., Anderson, G. and Palcic, B.: Image database system used for computer-aided teaching in cytology. 1st Int'l. Conference on Artificial Intelligence Systems, Los Angeles, February 1-3, 1987.

4. Jaggi, B., Massing, B., MacAulay, C., Poon, S.S.S. and Palcic, B.: Quantitative morphometric assessment of leukemic cells. 1st Int'l. Conference on Artificial Intelligence Systems, Los Angeles, February 1-3, 1987.

5. Jaggi, B., Poon, S.S.S., Pontifex, B.D., Deen, M.J. and Palcic, B.: Design and development of a solid state microscope for image cytometry. 4th Int'l. Cong. of Cell Biol., Montreal, Aug. 14-19, 1988.

6. Poon, S.S.S., Jaggi, B. and Palcic, B.: Colour segmentation of blood smears. 4th Int'l. Cong. of Cell Biol., Montreal, Aug. 14-19, 1988.

7. Palcic, B., Poon S.S.S. and Jaggi, B.: Recognition and analysis of live unstained cells. Digital Imaging Technology for Oncology, Terry Fox Workshop, Vancouver, B.C., October 19-22, 1988.

8. Poon, S.S.S., Ward, R.K., Beddoes, M.P. and Palcic, B.: Detection of leukocytes in Wright's stained cells. Digital Imaging Technology for Oncology, Terry Fox Workshop, Vancouver, B.C., October 19-22, 1988.

9. Jaggi, B., Poon, S.S.S., Pontifex, B., Fengler, J.P. and Palcic, B.: The development of a quantitative microscope for image cytometry. 1st Mtg. Eur. Soc. for Analyt. Cell. Path., Schloss Elmau, FRG, November 12-17, 1989.

10. Poon, S.S.S., Ward, R.K., Beddoes, M.P. and Palcic, B.: Detection and segmentation of nucleated cells in blood smears. 1st Mtg. Eur. Soc. for Analyt. Cell. Path., Schloss Elmau, FRG, November 12-17, 1989.

SCHOLARSHIPS AND AWARDS:

1985 University Scholarship, U.B.C.
1984 University Scholarship, U.B.C.
1983 Mackenzie Swan Memorial Scholarship
1980 B.C. Government Scholarship
Gold Lion Award (honour student in grades 10-12)
Book Proficiency Awards (top student in Electronics and Science)